P21: Spins of the Most Massive BBHs Observed by LIGO-Virgo-KAGRA

Soichiro Morisaki[1], Kenta Hotokezaka[2], Tomoya Kinugawa[3]. Kazuya Kobayashi[1]
[1]ICRR/UTokyo, [2]RESCEU/UTokyo [3]Shinshu University

Credit: LIGO-Virgo-KAGRA, arXiv: 2507.08219.

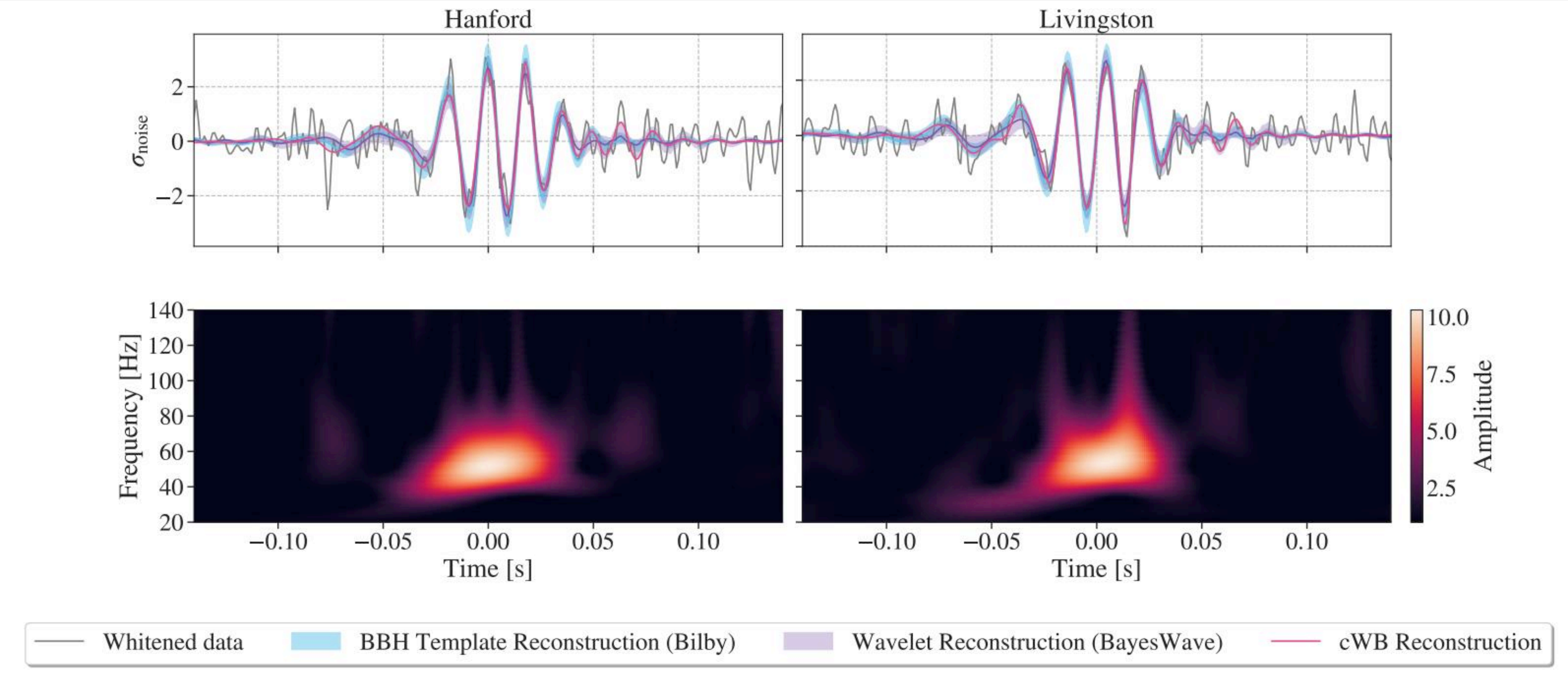

- A few massive ($m_1 > 80M_\odot$) BBHs observed by LIGO-Virgo-KAGRA (e.g. GW231123).
- Both BHs for GW231123 exhibit high spins ($0.90^{+0.10}_{-0.19}$ and $0.80^{+0.20}_{-0.52}$).

Can we increase our confidence that these events are truly circular binaries using multiple detections?

$$\vec{J} = \vec{L} + \vec{S}_1 + \vec{S}_2$$

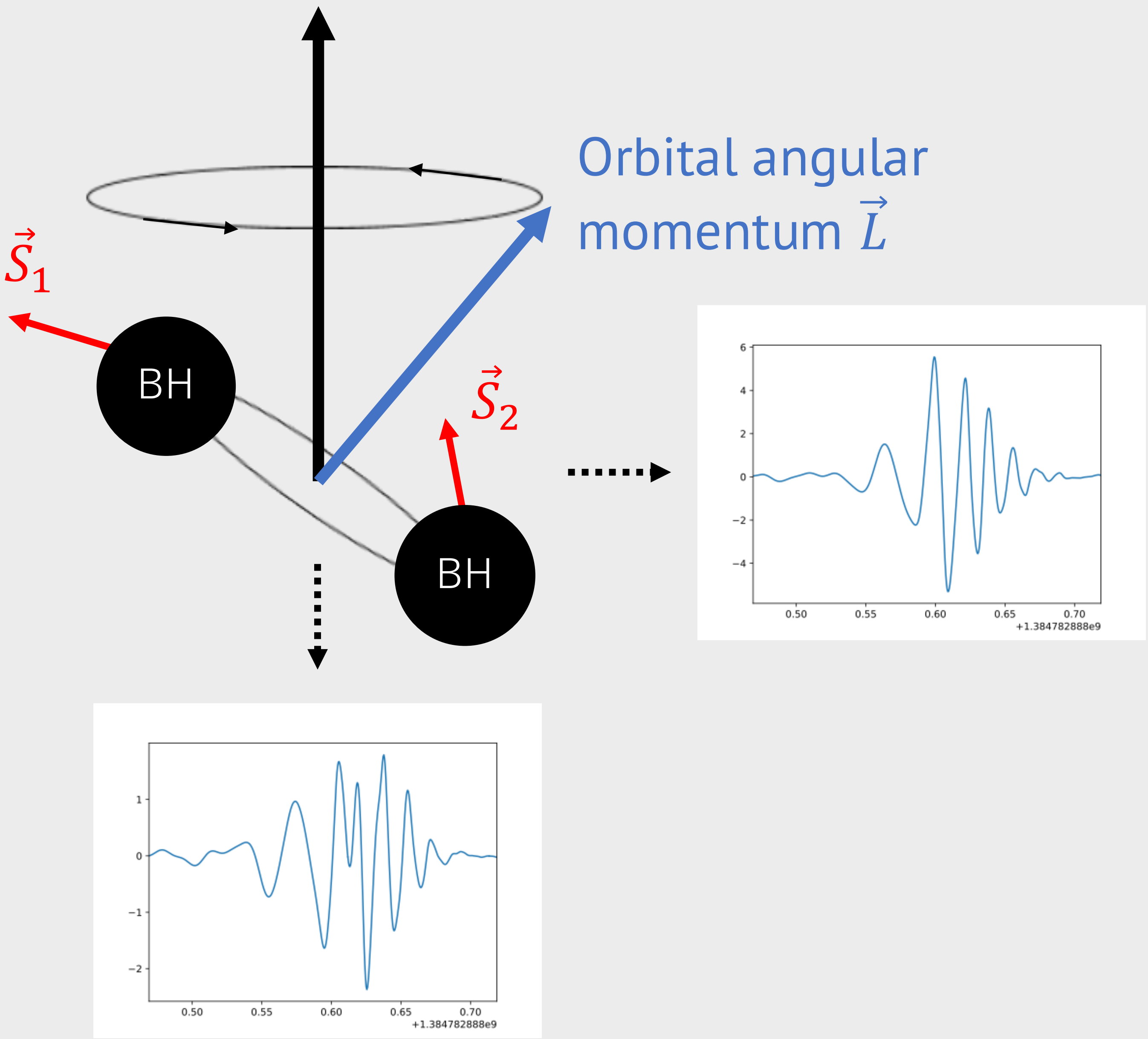

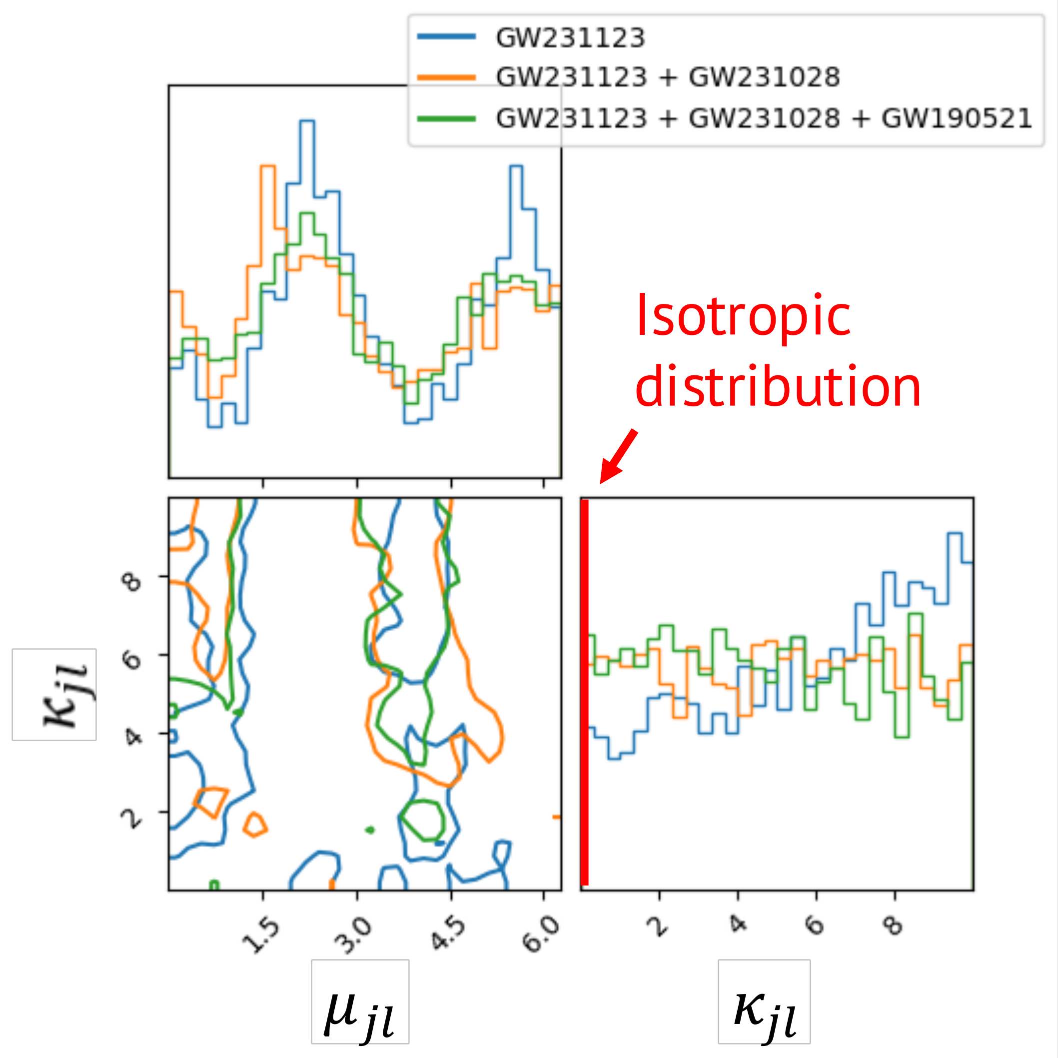

Figure: Results of hierarchical Bayesian inference testing whether binary orientations are isotropically distributed

P22

Simulating Binary Neutron Star Mergers and their Multi-Messenger Signals

The Influence of Spin

arXiv: 2510.14850
(accepted in PRD)

A. Neuweiler, H. Gieg, H. Rose, H. Koehn, I. Markin, F. Schianchi, L. Brodie, A. Haber, V. Nedora, M. Bulla, and T. Dietrich

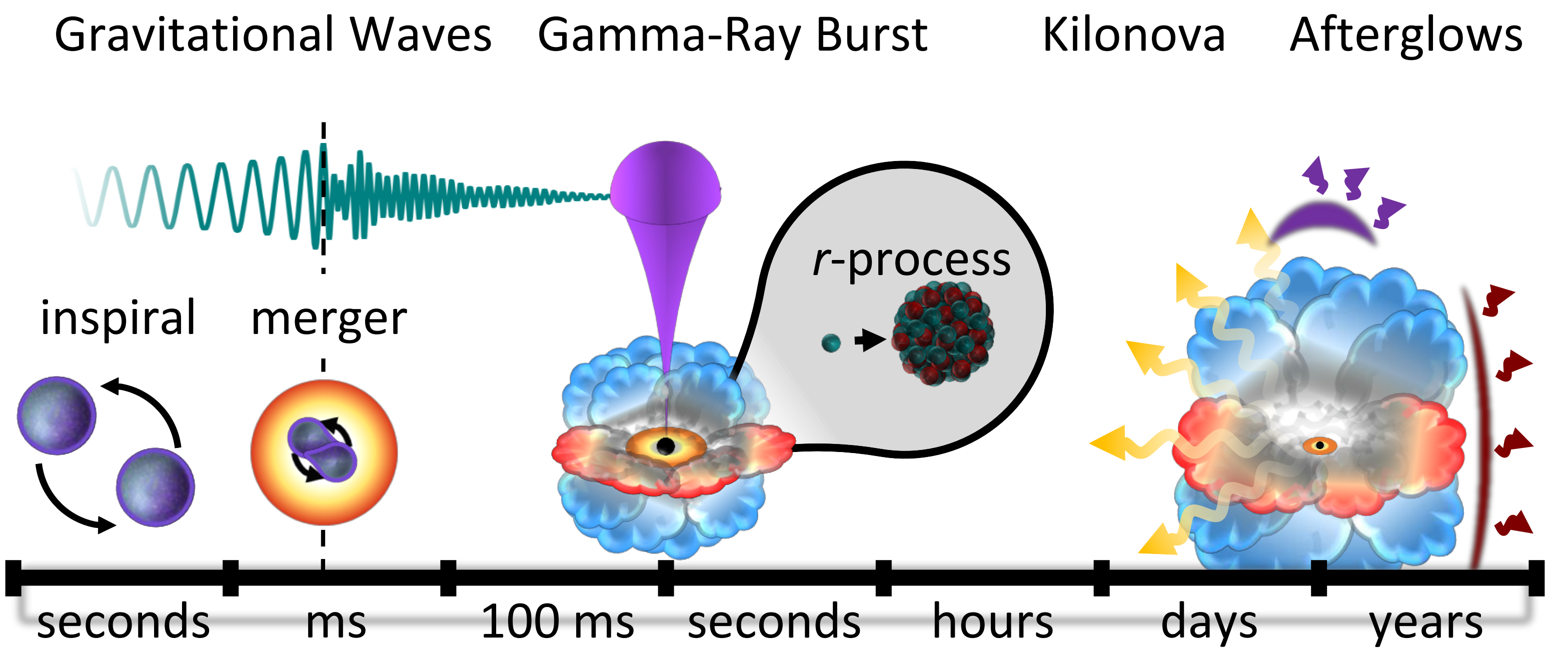

Codes for Simulations & Post-Processing

BAM – Numerical-Relativity Code
- magnetic fields
- M1 neutrino transport

WinNet – Nuclear-Reaction Network

POSSIS – Radiative Transfer Code

PyBlastAfterglow – Semi-Analytic

Binary Neutron Star Systems

- $M_1 = M_2 = 1.35\ M_\odot$
- ABHT (QMC-RMF3)
- R1 ~ 190 m / R2 ~ 95 m

➢ **non-spinning** $\chi_1 = \chi_2 = 0.0$
➢ **aligned-spin** $\chi_1 = \chi_2 = 0.1$

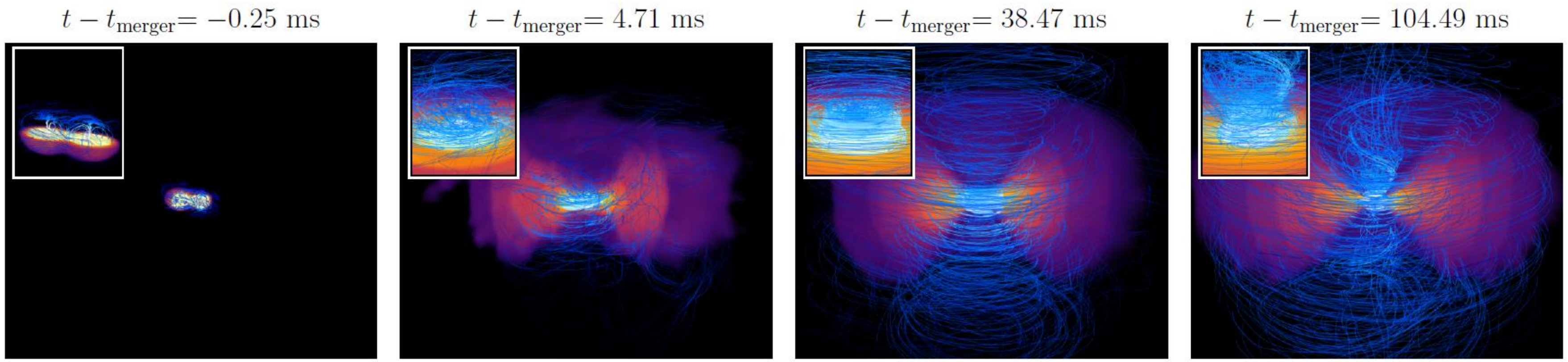

Nuclear Abundances

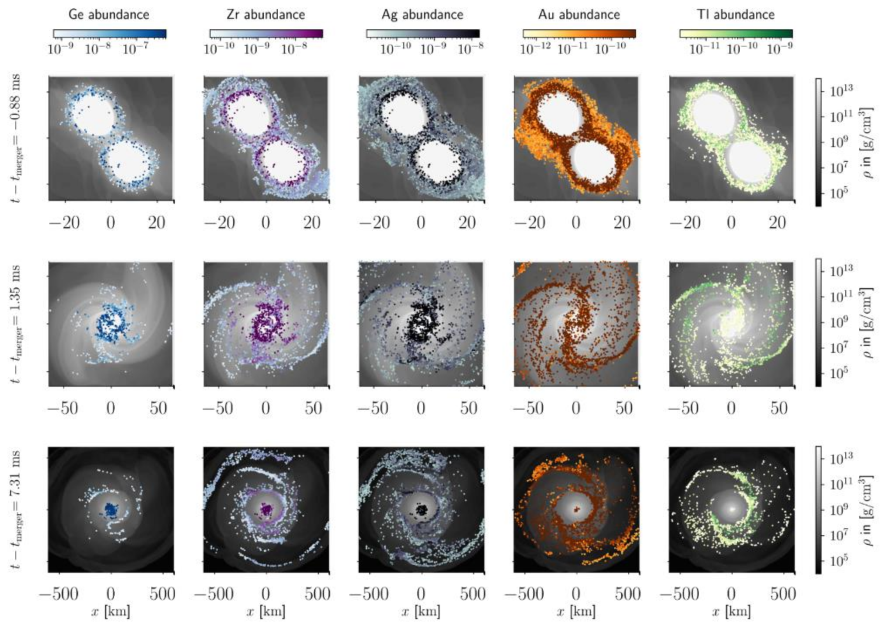

Multi-Messenger Picture

Gravitational Waves

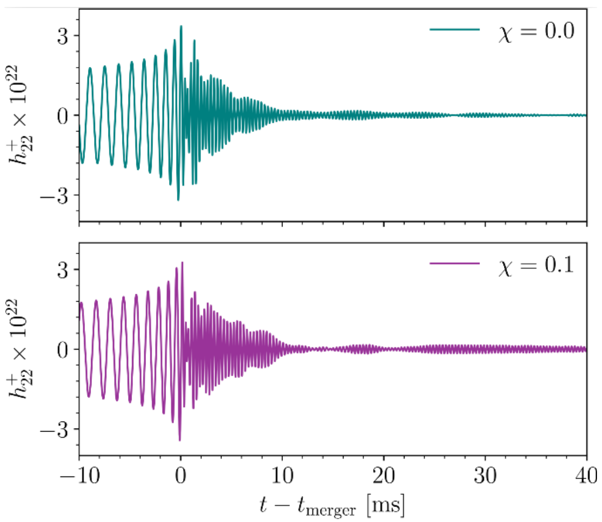

Kilonova

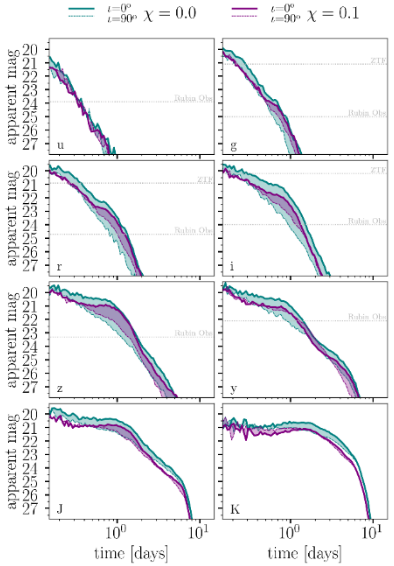

Afterglows

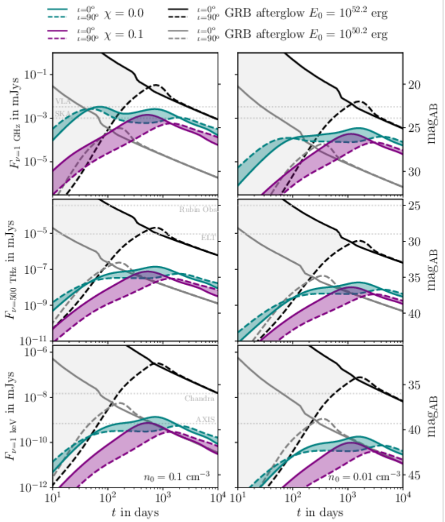

P24

The M-σ Relation Has To Break

Omri Nitzan & Re’em Sari

האוניברסיטה העברית בירושלים
THE HEBREW UNIVERSITY OF JERUSALEM

מכון רקח
The Racah Institute
לפיסיקה
of Physics

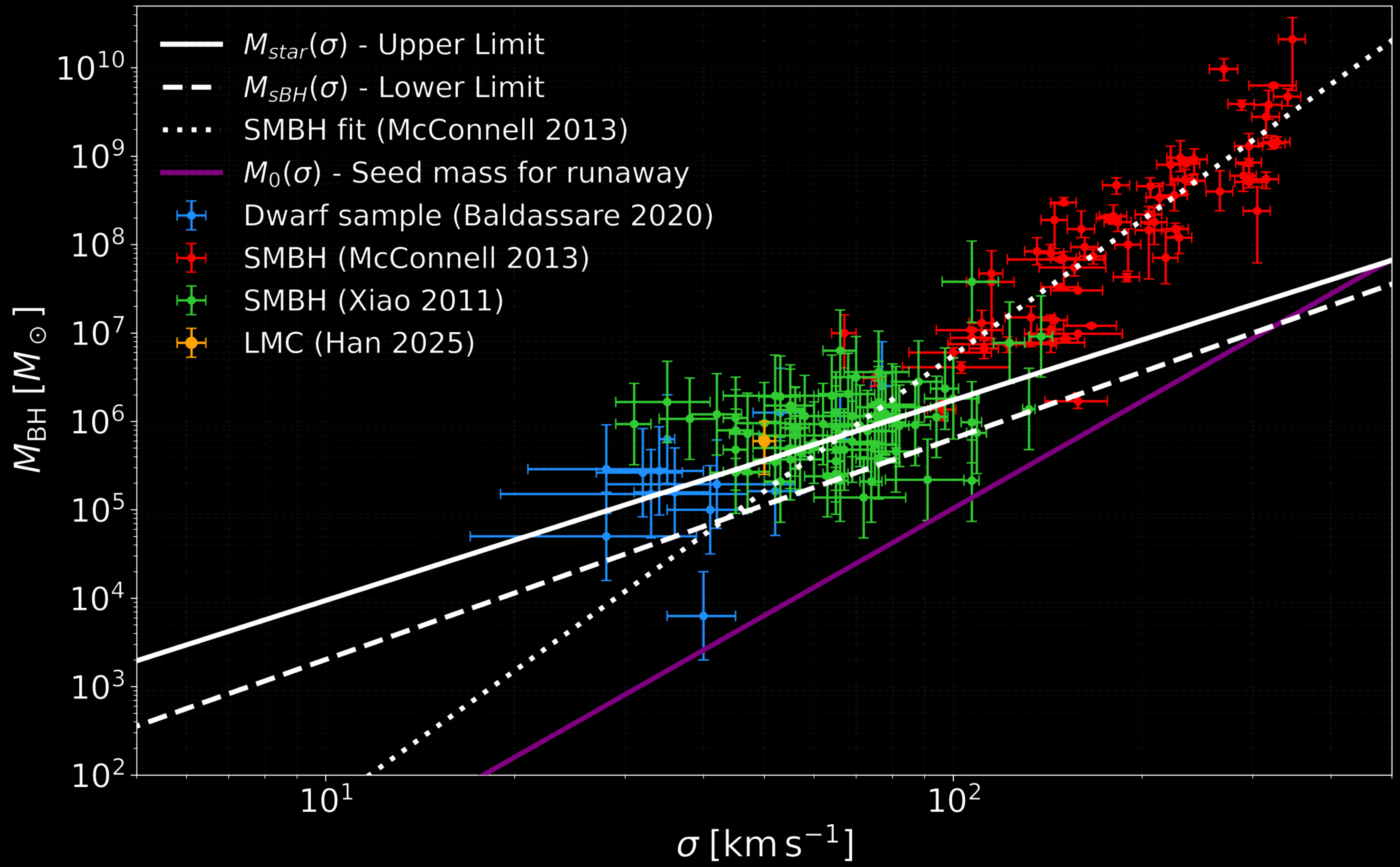

$M_{star}(\sigma)$ - Upper Limit
$M_{sBH}(\sigma)$ - Lower Limit
SMBH fit (McConnell 2013)
$M_0(\sigma)$ - Seed mass for runaway
Dwarf sample (Baldassare 2020)
SMBH (McConnell 2013)
SMBH (Xiao 2011)
LMC (Han 2025)
$M_{\rm BH}\ [M_\odot]$
$\sigma\ [\rm km\,s^{-1}]$
10^{2}
10^{3}
10^{4}
10^{5}
10^{6}
10^{7}
10^{8}
10^{9}
10^{10}
10^{1}
10^{2}

P25

Different Stars, Different Kicks:

Natal Kick Segregation in High-Mass X-ray Binaries

Pornisara **(Grace)** Nuchvanichakul (U of Southampton, UK)

Collaborated with Poshak Gandhi, Christian Knigge, Yue (Cory) Zhao, and Cordelia Dashwood Brown

High-Mass X-ray Binaries

- Consist of a compact object that is accreting material from a massive companion
- Over 100 systems in the Milky Way
- Excellent tools for probing Galactic star formation and accretion onto compact objects

Kicks


Credit: NASA/ESA/G. Bacon, STScI

- Impulse imparted to remnant at the instant of supernova explosion (Belczynski+16)
- symmetric mass-loss (e.g. Blaauw+61)
- asymmetric ejecta in the supernova explosion (Janka+17)
- Peculiar velocity can be used to estimate kick

HMXB Subclasses


Credit: NASA/CXC/M. Weiss

OB Supergiant X-ray binaries (SgXRBs)

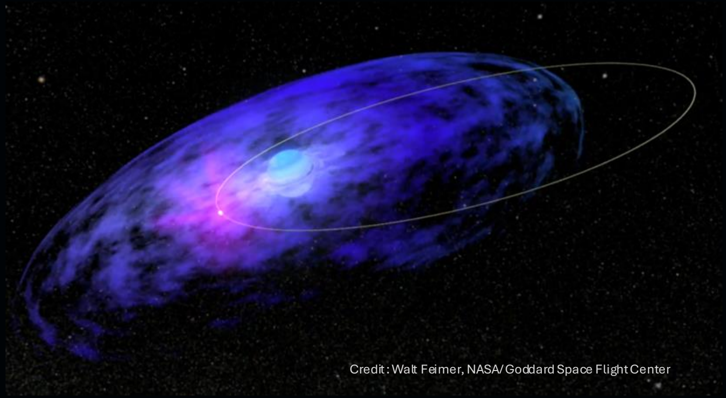
Credit: Walt Feimer, NASA/Goddard Space Flight Center

Be/X-ray binaries (BeXRBs)

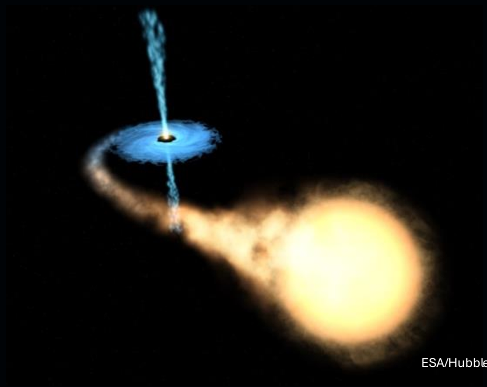
ESA/Hubble

Roche-lobe overflow HMXBs

Different Stars, Different Kicks:

Natal Kick Segregation in High-Mass X-ray Binaries

Board no: 25

Find me around during the poster session
and pop over with your questions!

Target selection

- X-ray binary catalogues (Neumann+23)
- Select reliable counterparts $\frac{\sigma_\pi}{\pi} < 20\%$ (Bailer-Jones05)
- Verify magnitude, finding charts, offsets of coordinate

Kinematics

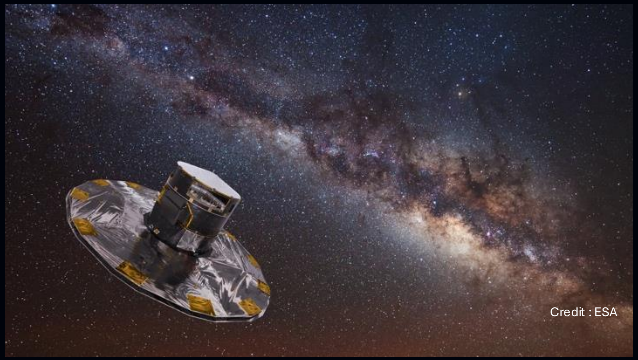

Astrometric parameters:

- position: α, δ
- proper motion: μ_α, μ_δ
- parallax: π

+ Systemic velocity

Reid+09

Peculiar Velocity: $V_{\rm pec}$

Results

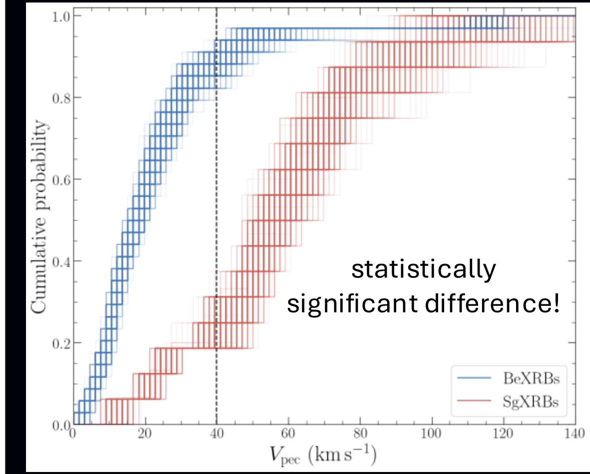

- Using a K–S test, we found the two datasets are unlikely to be drawn from the same distribution
- approximate division at $V_{\rm pec}$ of 40 $\rm km\,s^{-1}$

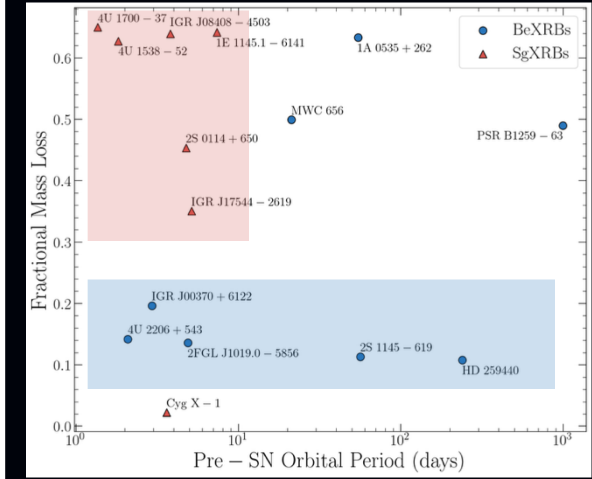

- Used COSMIC (BSE pop. synth.; Breivik+20) to study these effects
- SgXRBs favor shorter periods and higher fractional mass loss (different evolutionary pathways)

Pornisara Nuchvanichakul et al., Further evidence for natal kick segregation by spectral type in high-mass X-ray binaries, MNRAS, 543, 2, 2025, p. 1705

Achromatic and Delayed Gamma-ray burst afterglows from Relativistically moving thick-shell

Kaori Obayashi et al., in prep.

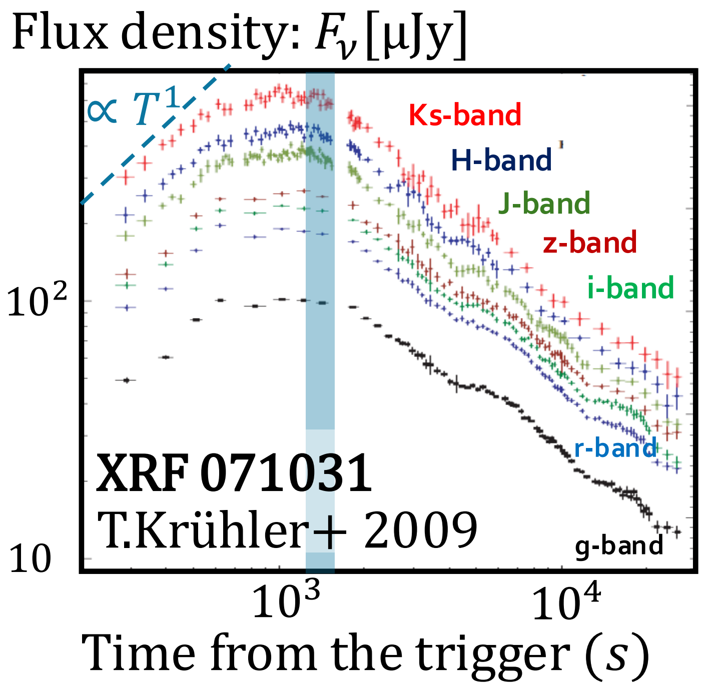

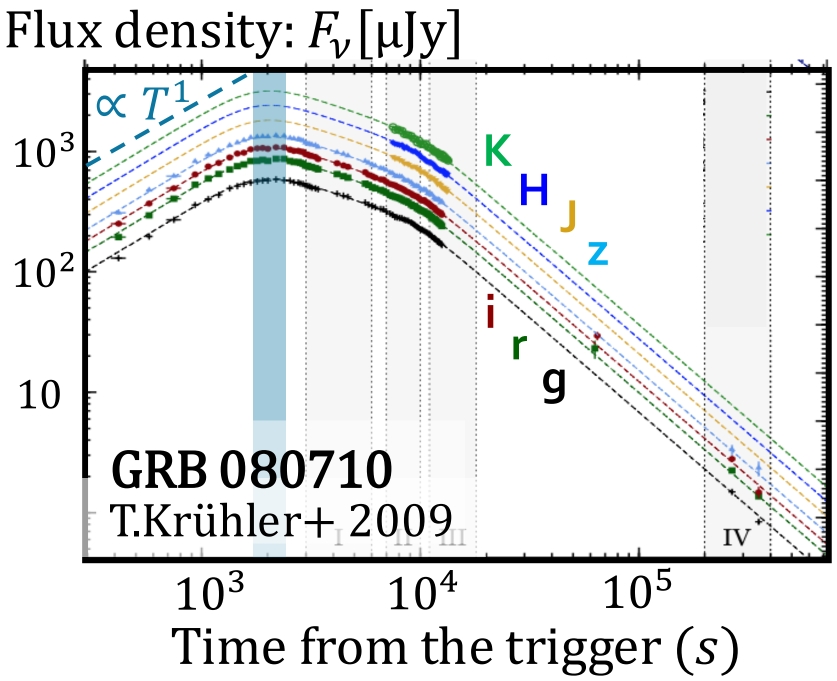

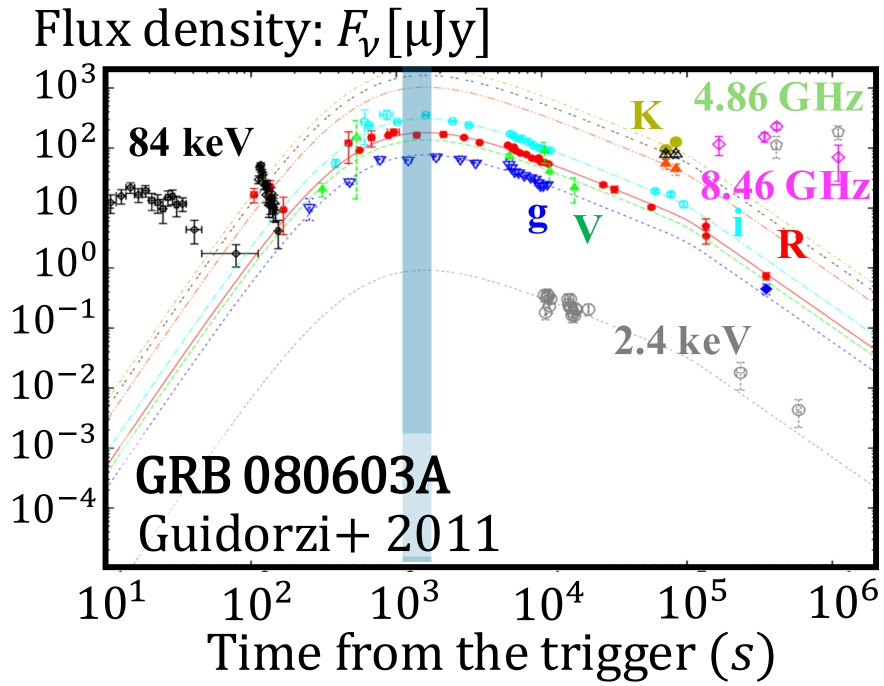

Some GRB afterglows in optical/IR show an achromatic peak at late times ($\sim 10^3$s from the trigger time).

Result: For GRB 080710 and XRF 080330, Bayesian inference **disfavors off-axis models** and **favors a dynamical origin** of the achromatic peak.

Forward shock dynamics: $\Gamma(R)$

e.g.) Yi+2013, Kusafuka+(2025a, b),

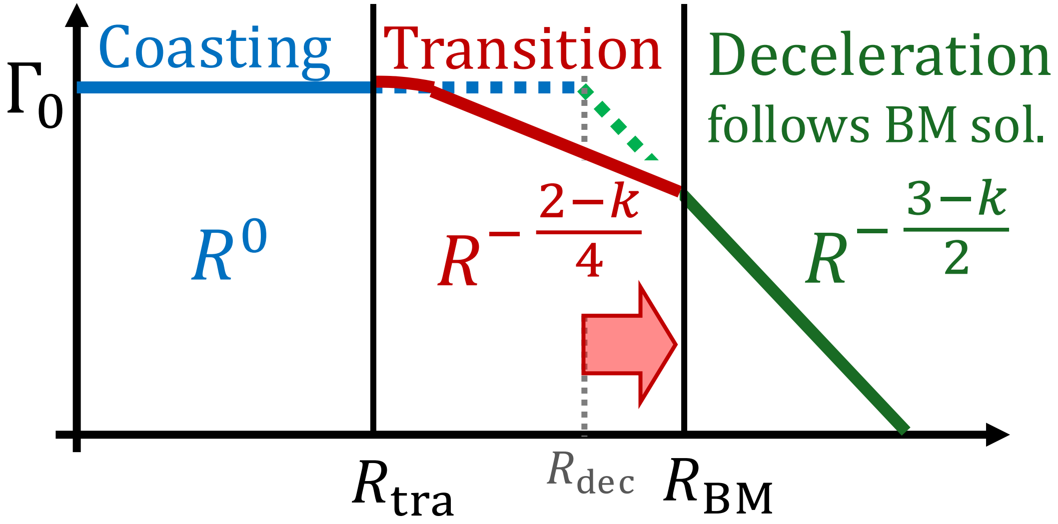

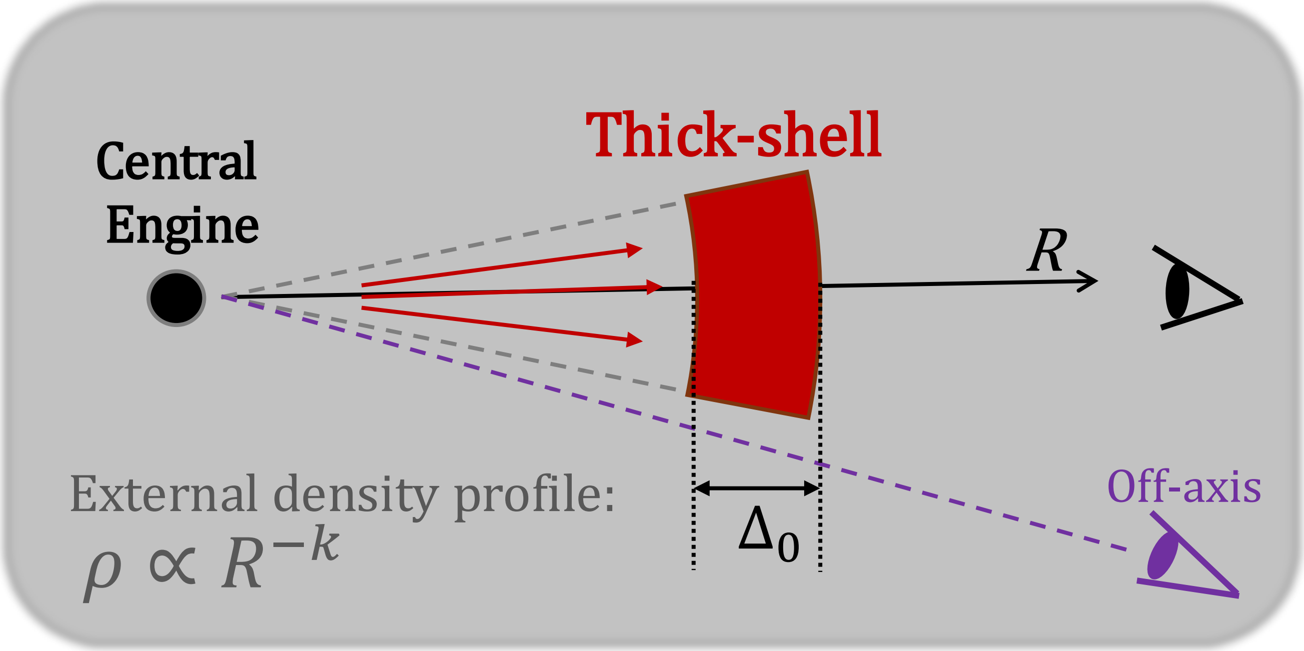

Implication: Central engine activity time $\Delta_0/c \sim \mathbf{10} \times T_{90}/(1+z)$

* T_{90} is prompt gamma duration. z is redshift.

YUKAWA INSTITUTE FOR THEORETICAL PHYSICS

The Reconstruction of Equation of State From Neutron Star Observables

By N. K. Patra (CUHKSZ,China)

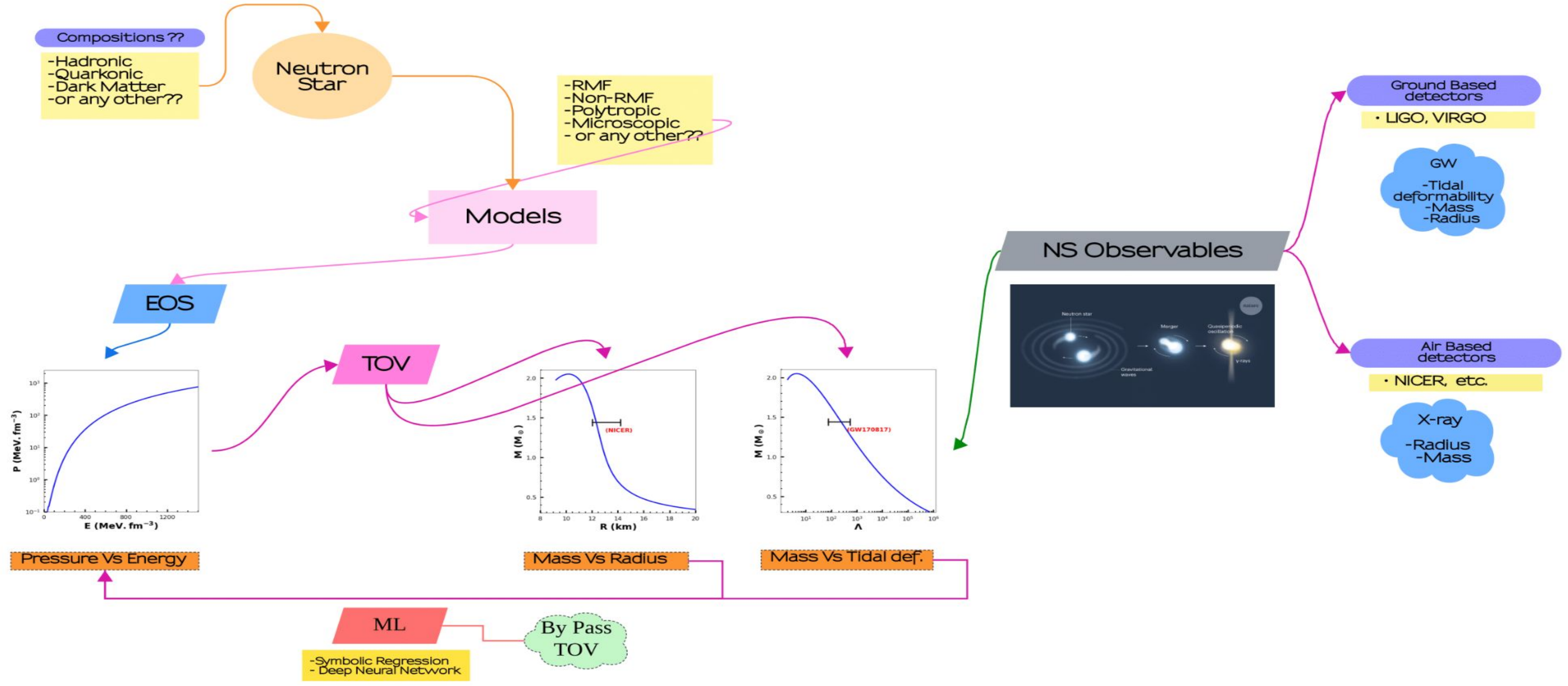

Some Important Results

Please visit : ***Phys.Lett.B*** **865 (2025) 139470 [arXiv: 2502.20226]**

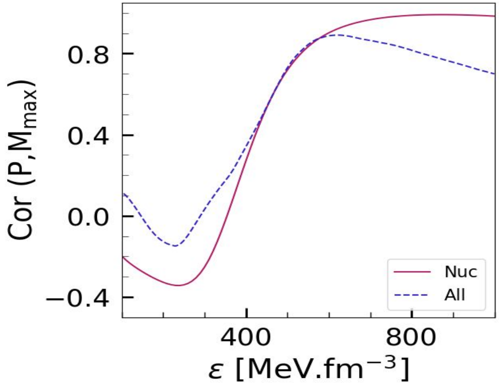

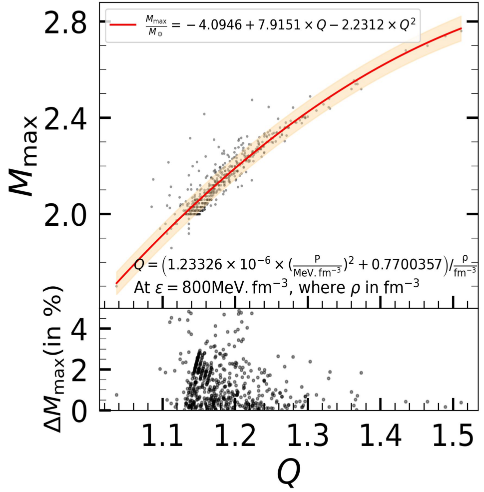

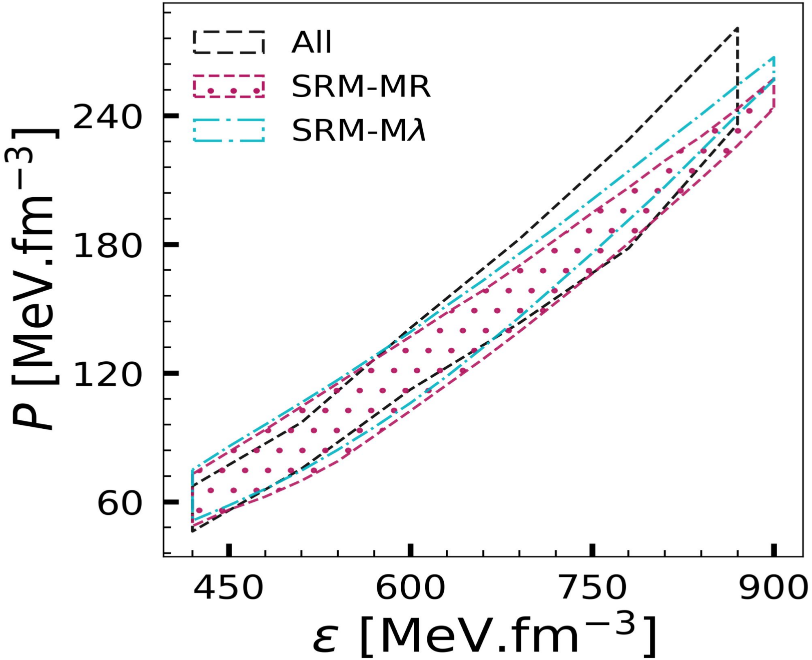

$$\frac{\epsilon}{\mathrm{MeV \cdot fm^{-3}}} = \frac{15500\left(\left(\frac{M}{M_\odot}\right)^3 + 1.018\left(\frac{M}{M_\odot}\right)^2 + \frac{M}{M_\odot}\right)}{\left(\frac{R}{\mathrm{km}}\right)^2} - \frac{3100\left(\frac{R}{\mathrm{km}}\right)\left(\frac{M}{M_\odot}\right)^2 + 46747.711}{\left(\frac{R}{\mathrm{km}}\right)^2}, \quad (4)$$

$$\frac{P}{\mathrm{MeV \cdot fm^{-3}}} = \frac{5 \times 10^{5.540} \times 10^{\left(\frac{M}{M_\odot}\right)}}{\left(\frac{R}{\mathrm{km}}\right)^{5.540}} + 18.553. \quad (5)$$

GWs from Strongly Magnetized Eccentric Neutron Star Binaries

- Prasad R (ICTS), Anushka Doke (UMass), Prayush Kumar (ICTS) arXiv:2508.08234v2

We are shifting from an era of **first discoveries to high-precision astronomy.**

- ET/CE: $f_{start} = 5\,\text{Hz}$ to $f_{end} = f_{ISCO}$
- DECIGO: $f_{start} = 10^{-1}\,\text{Hz}$ to $f_{end} = 10\,\text{Hz}$

Long inspirals, High SNRs

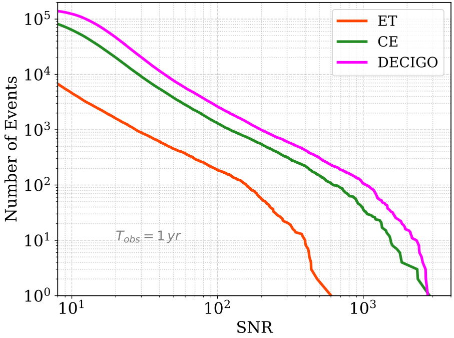

Magnetic Effects:
Magnetic Interaction + EM Emission

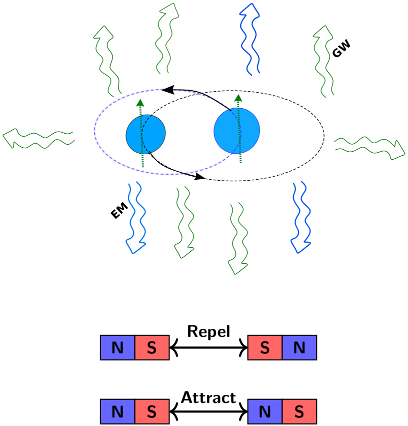

GWs from Strongly Magnetized Eccentric Neutron Star Binaries

- Prasad R (ICTS), Anushka Doke (UMass), Prayush Kumar (ICTS) **arXiv:2508.08234v2**

Horizon Distance

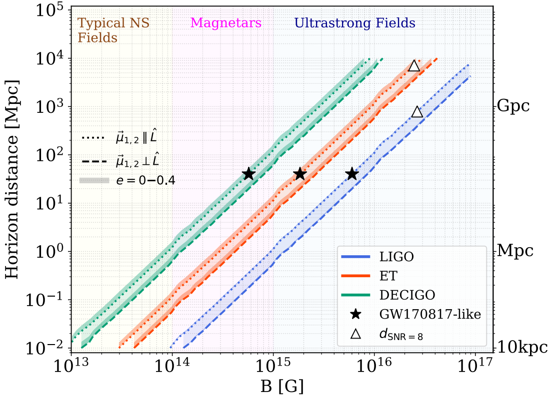

Measurement Prospects

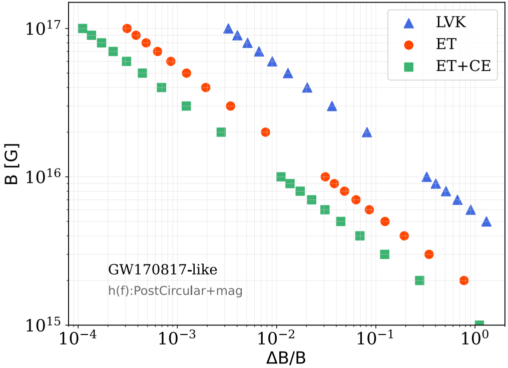

Magnetar-level fields or higher may be distinguishable in GWs.

Modeling the late spectra of energetic supernovae

Giacomo Ricigliano, Kenta Hotokezaka, Almudena Arcones

Max-Planck-Institut für Kernphysik

Technische Universität Darmstadt

Poster # 29

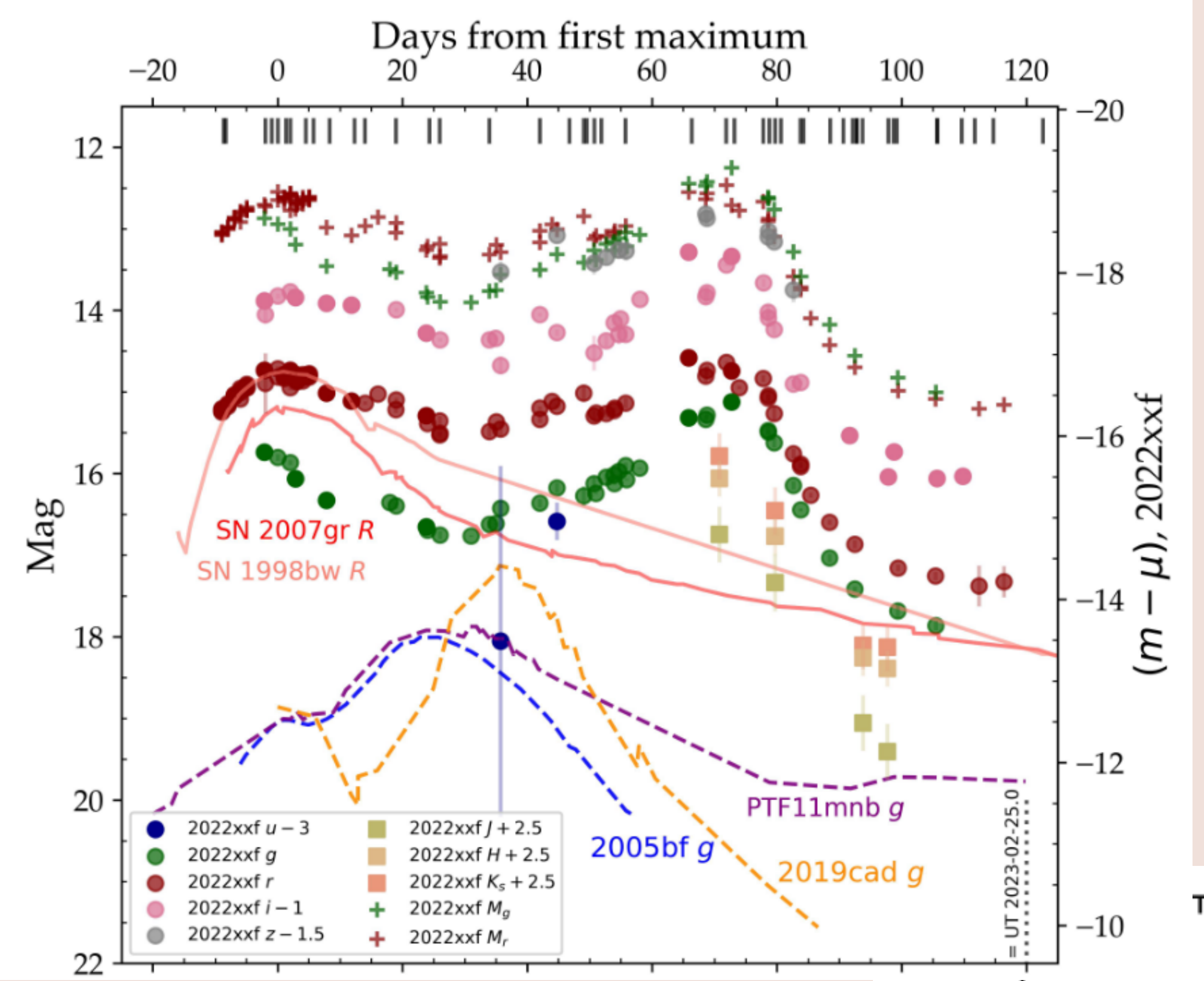

Kuncarayakti et al. 2023, A&A 678

By now several observed energetic and peculiar events

(e.g. GRB SNe, Type Ic BL, SLSNe I...)

Milisavljevic et al. 2018, ApJ 864

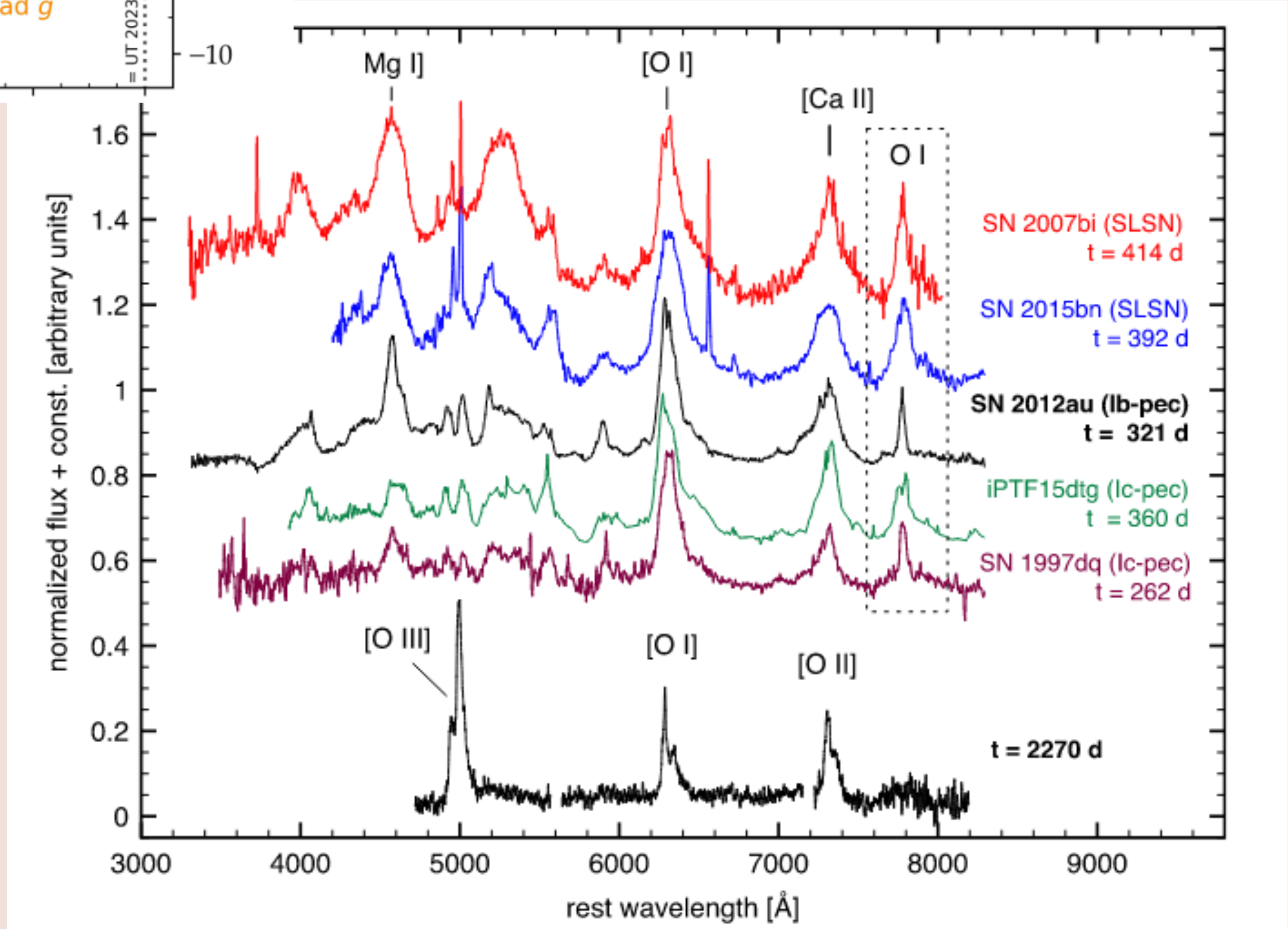

Models for mechanisms are still largely unconstrained

Engine traces in the ejecta extend to the **nebular phase**

when all the ouflow is scanned

Plasma solver

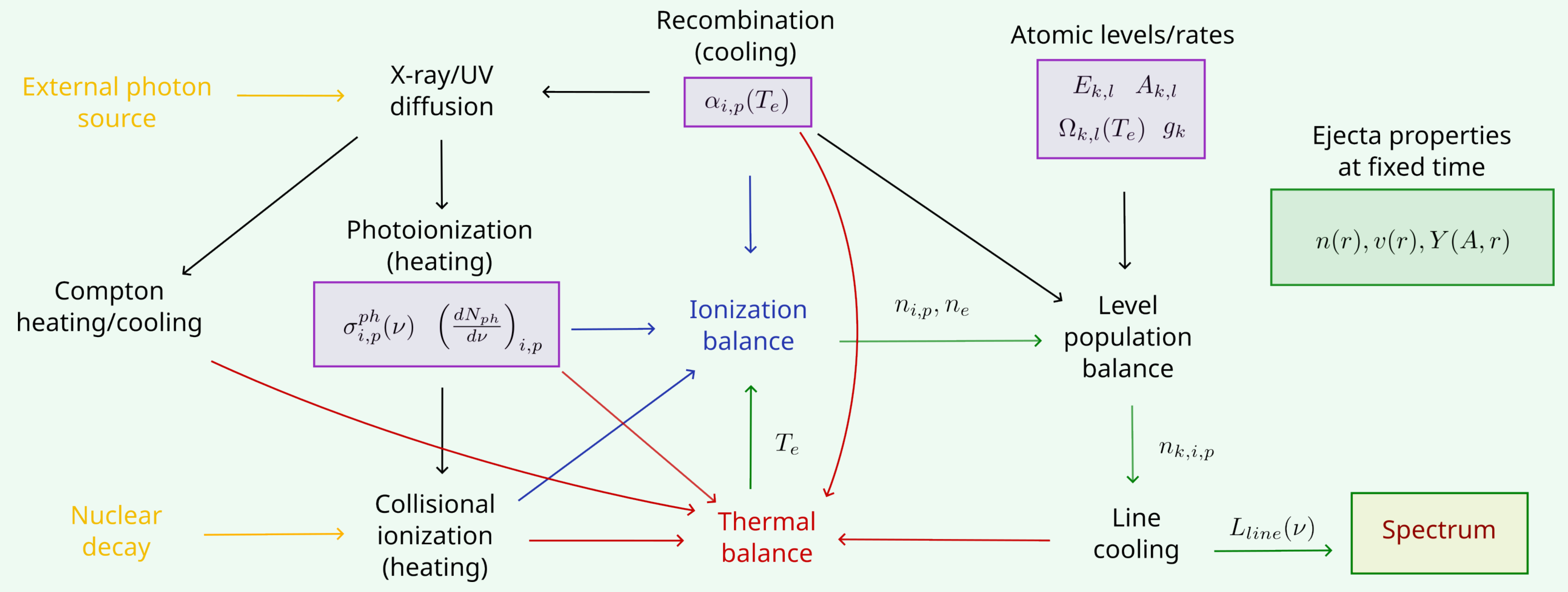

Modeling the late spectra of energetic supernovae

Giacomo Ricigliano, Kenta Hotokezaka, Almudena Arcones

Max-Planck-Institut für Kernphysik

Technische Universität Darmstadt

Poster # 29

Target questions:

Could the presence of heavy elements from r-process be detected in the SN nebular phase?

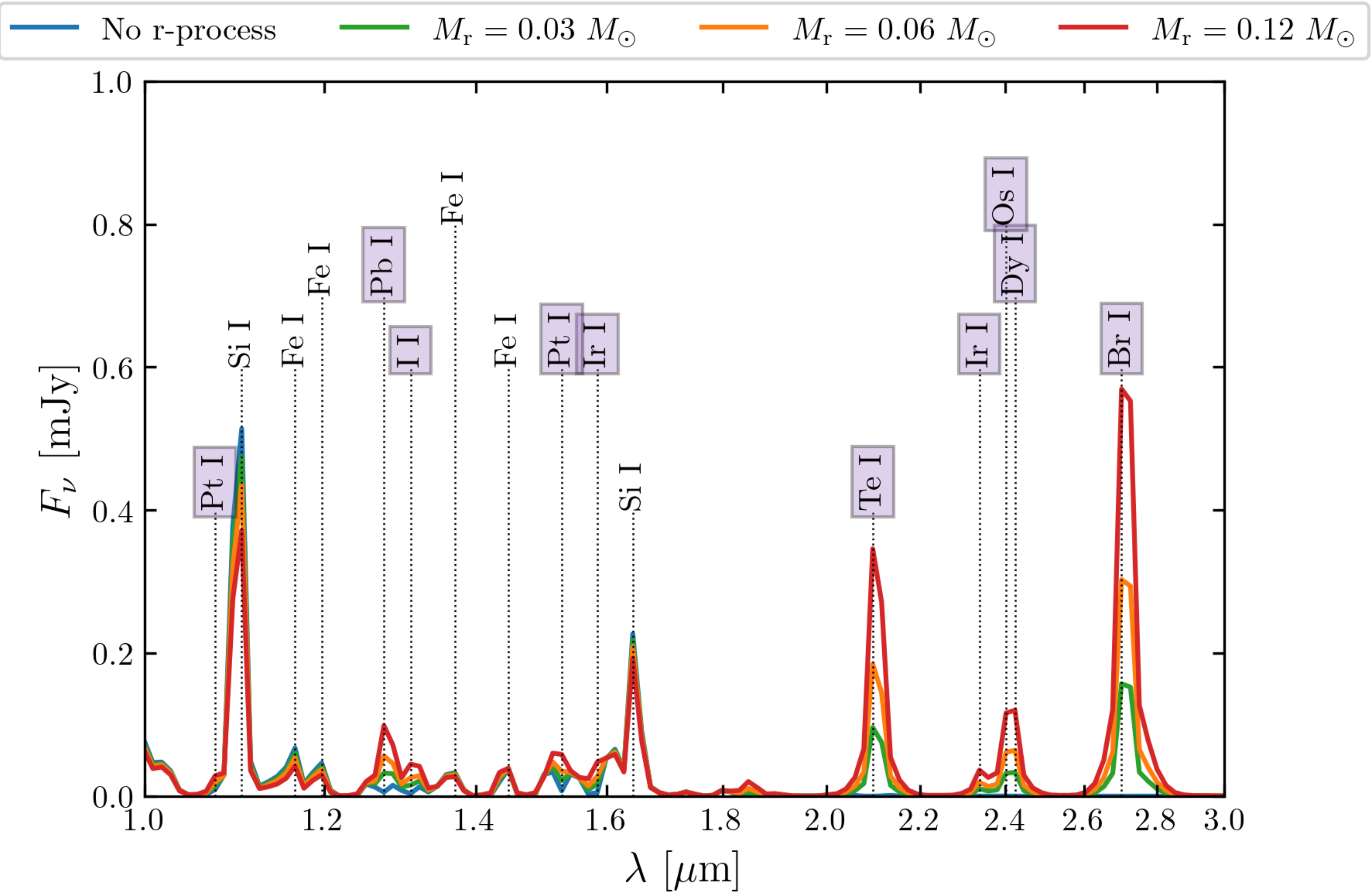

Ricigliano, Hotokezaka & Arcones 2025, MNRAS 543

How much can optical+IR nebular spectra help in constraining powering mechanism?

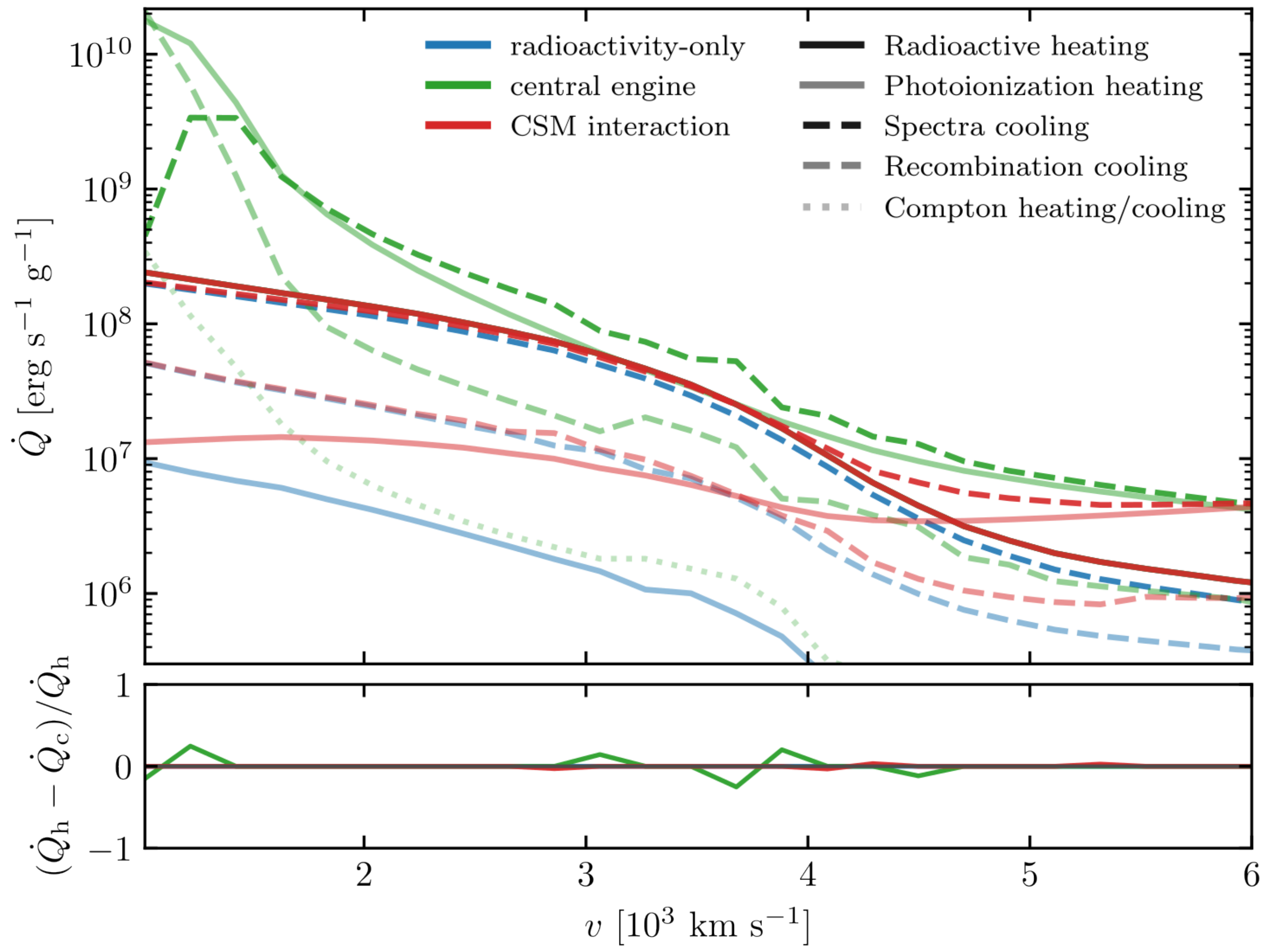

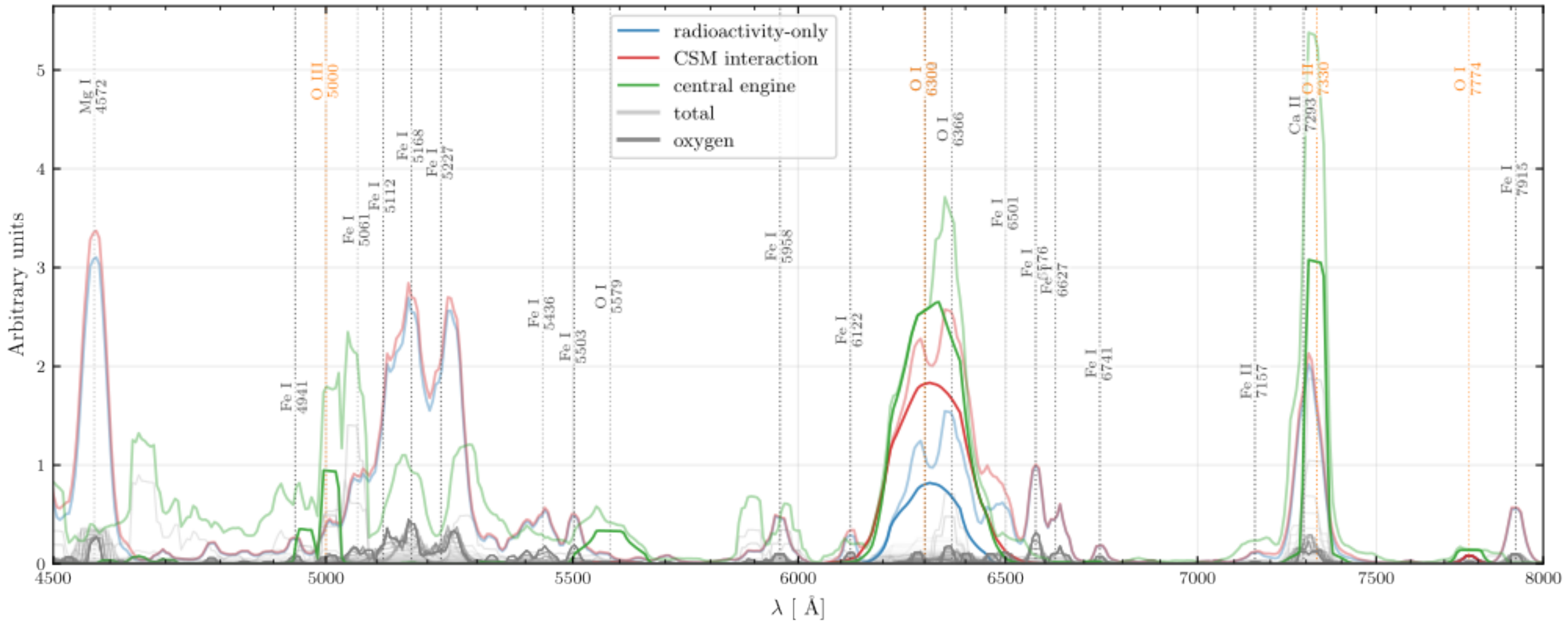

GRB X-ray plateaus from stratified ultra-relativistic outflows

Gilad Sadeh — Kenta Hotokezaka — Masaru Shibata , Poster #30

MAX PLANCK INSTITUTE FOR GRAVITATIONAL PHYSICS (Albert Einstein Institute)

Hydrodynamics: ultra-relativistic ($\gamma \gtrsim 100$) outflows associated with the prompt γ-ray emission are expected to have a continuous distribution of Lorentz factors, $M(>\gamma) \propto \gamma^{-s}$, within the ejecta.

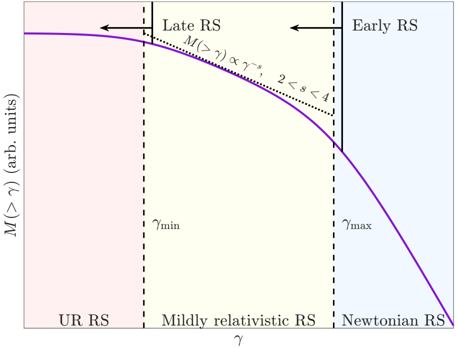

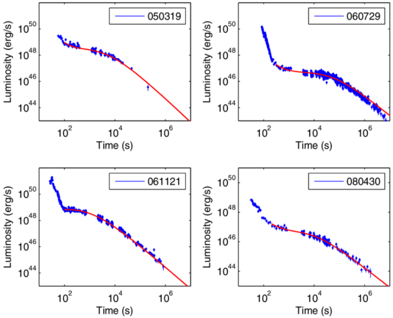

For moderate values of $2 \lesssim s \lesssim 4$, the reverse shock is mildly relativistic, and its ejecta crossing time is significantly ($\sim$ factor of 5–10) larger than the typical crossing time obtained in the thin shell case.

GRB X-ray plateaus from stratified ultra-relativistic outflows

Gilad Sadeh — Kenta Hotokezaka — Masaru Shibata , Poster #30

MAX PLANCK INSTITUTE FOR GRAVITATIONAL PHYSICS (Albert Einstein Institute)

Synchrotron emission: relativistic electrons in the shocked regions emit radiation $F_\nu \propto t^{-\alpha}\nu^{-\beta}$.

The forward shock naturally produces a shallow, long-lasting X-ray decay consistent with the observed properties of X-ray plateaus, $F_\nu \propto t^{-0.5}$ for $\nu > \nu_c^f$. After the crossing time, typical $F_\nu \propto t^{-1.2}$ is expected.

Representative broadband synchrotron spectra at $t \simeq 1$ hr for fiducial parameters.

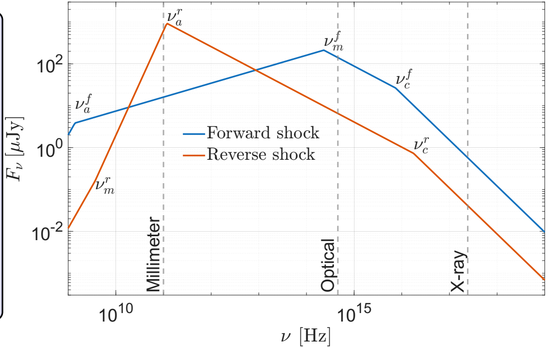

The reverse shock generates a long-lived millimeter emission component that out-shines the forward shock emission at these wavelengths, $\nu = \nu_a^r$. After the crossing time, the mm emission will terminate smoothly.

No need to invoke a long-lived central engine, an energetic low γ outflow, or a fine-tuned viewing angle.

WHAT HAPPENS WHEN NEUTRON STAR SPINS DOWN?

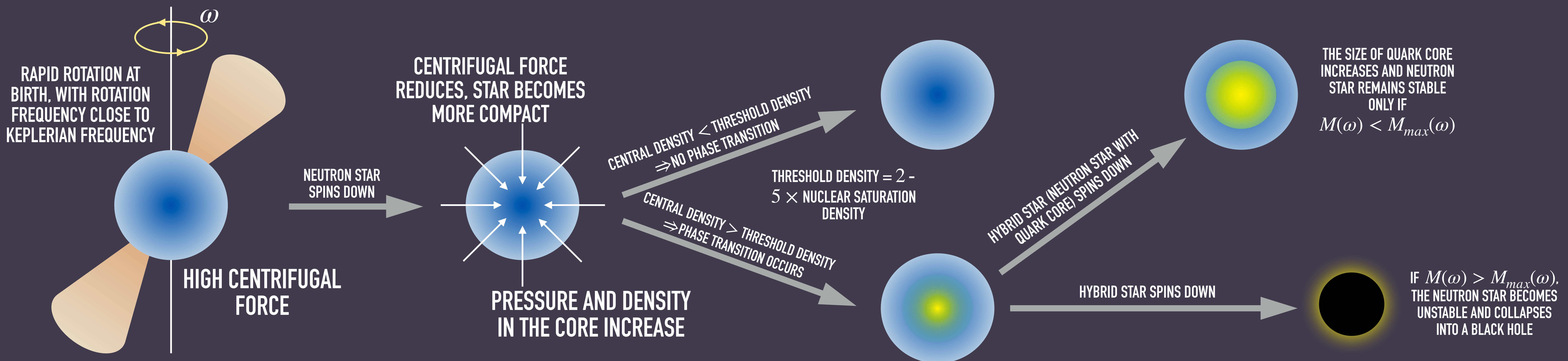

CHECK OUT MY POSTER!!
POSTER NO. 31

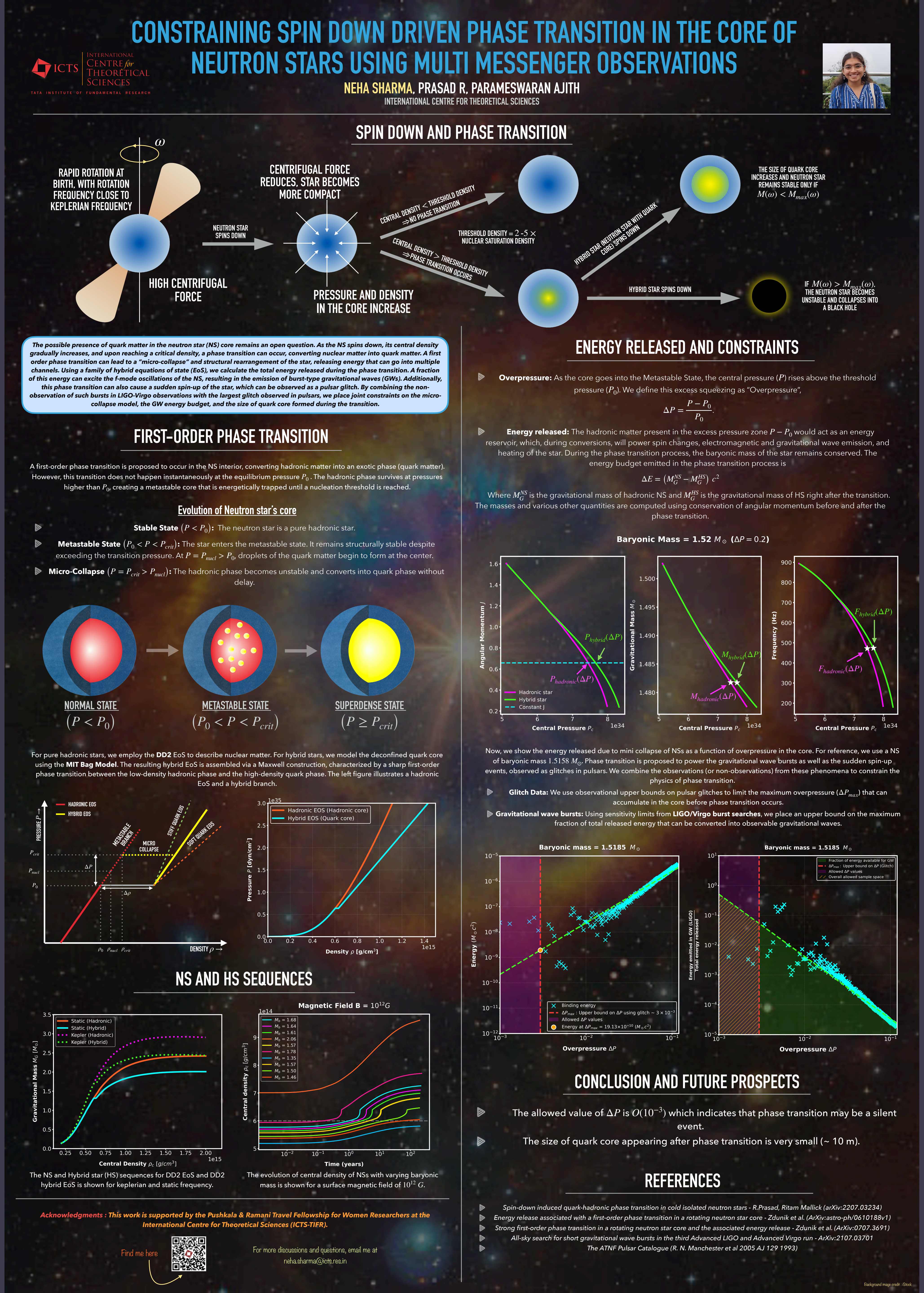

Dust Formation in Failed Supernova

Kengo Shinoda, Ryo Tazaki, Takato Tokuno, Yudai Suwa (Univ. of Tokyo)

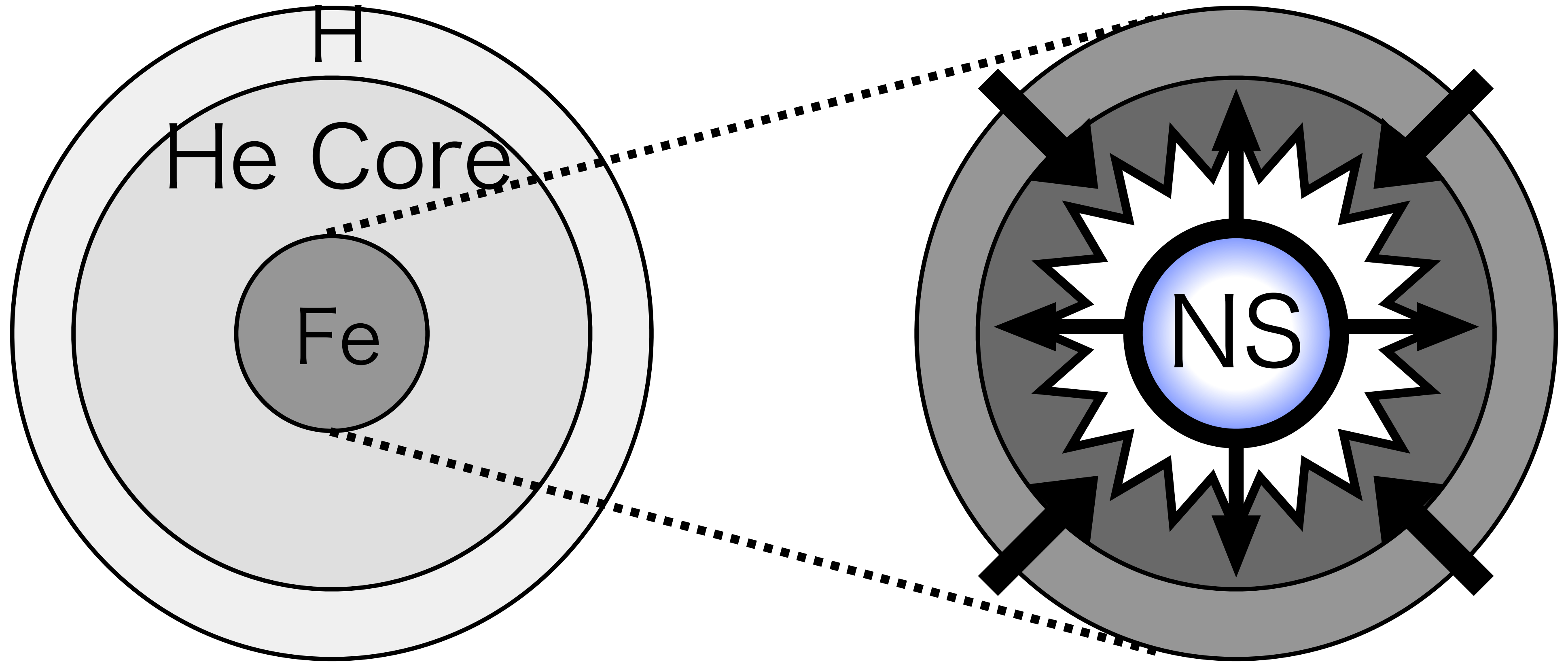

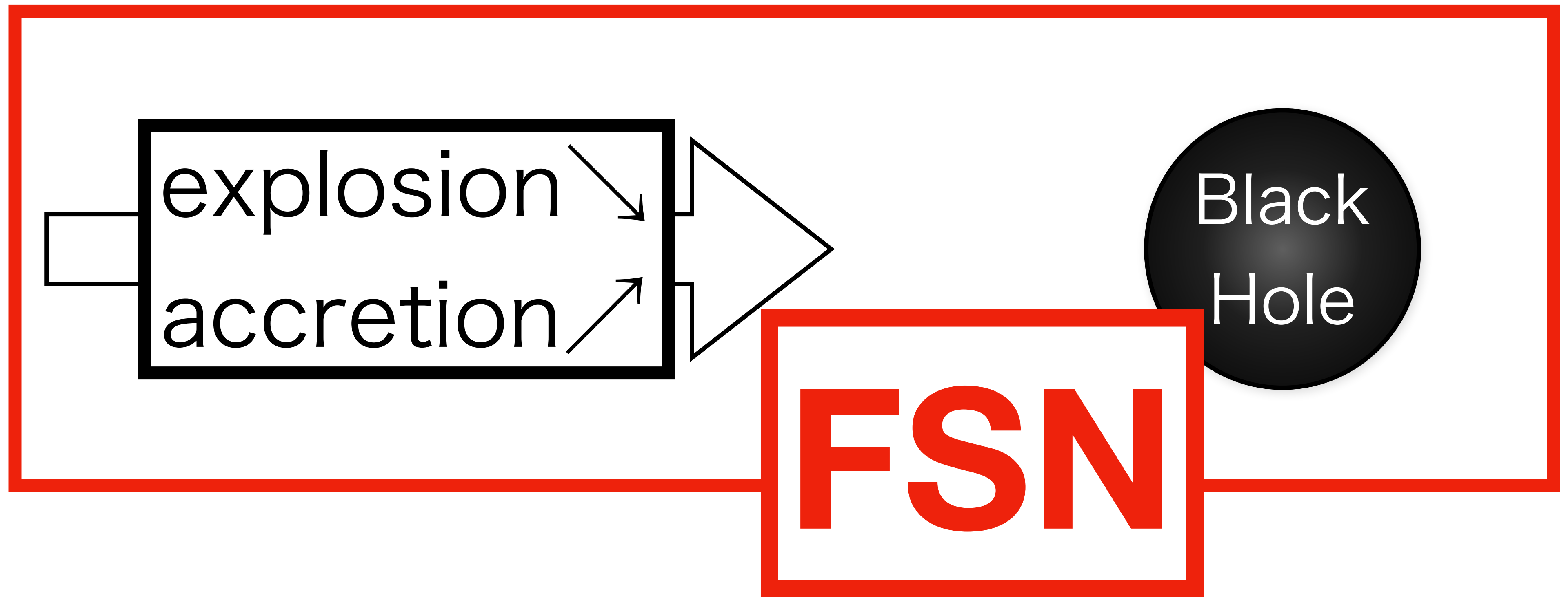

- Candidate: **M31-2014-DS1**

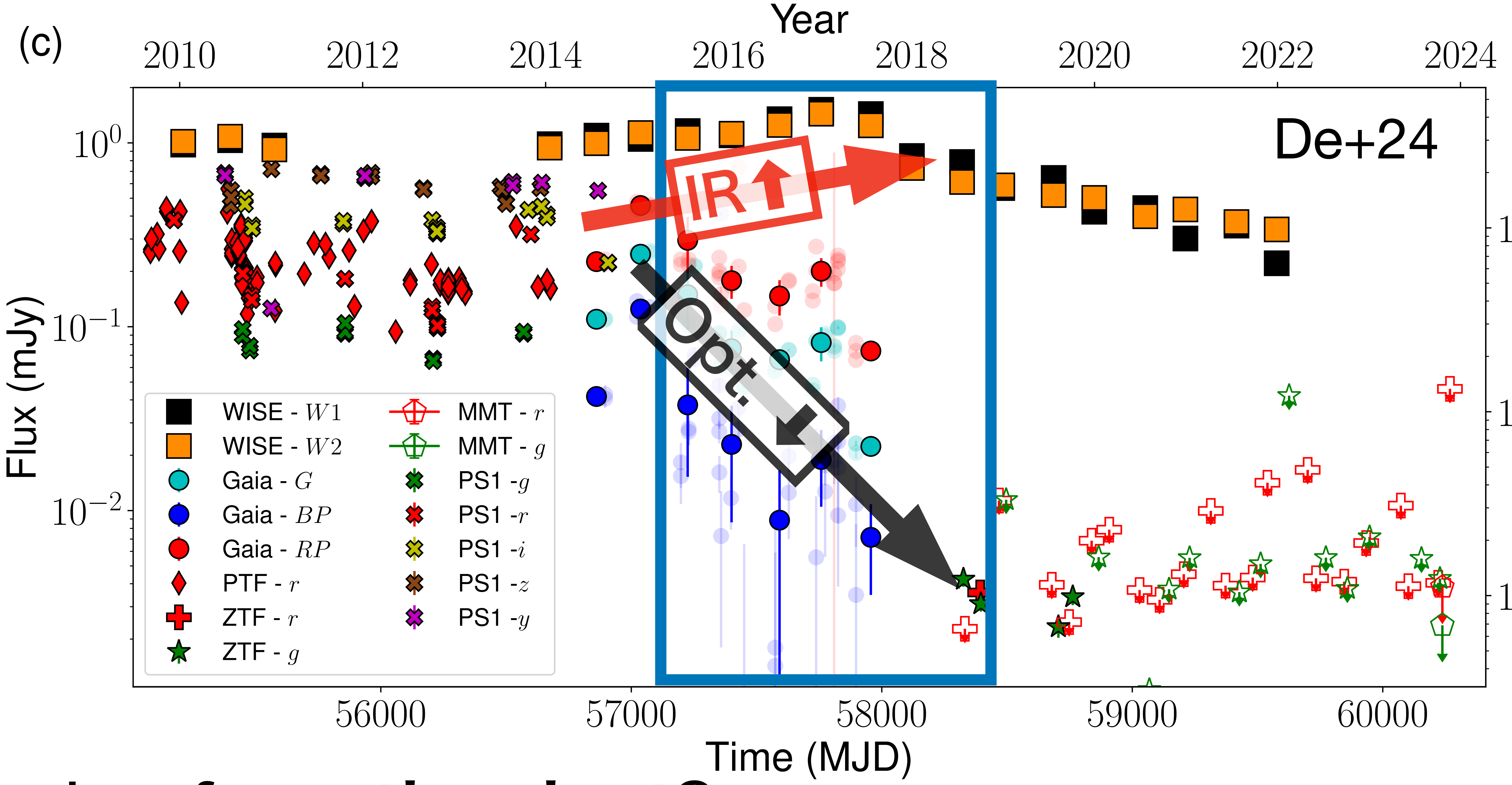

- Opt. ⬇, IR⬆ ⇒ the thermal emission from **the dust**?
- **Dark FSN:** IR afterglow = the only tracer to observe BH formation in FSN
- We need **the time evolution** of dust properties for the LC!

Dust Formation in Failed Supernova

Kengo Shinoda, Ryo Tazaki, Takato Tokuno, Yudai Suwa (Univ. of Tokyo)

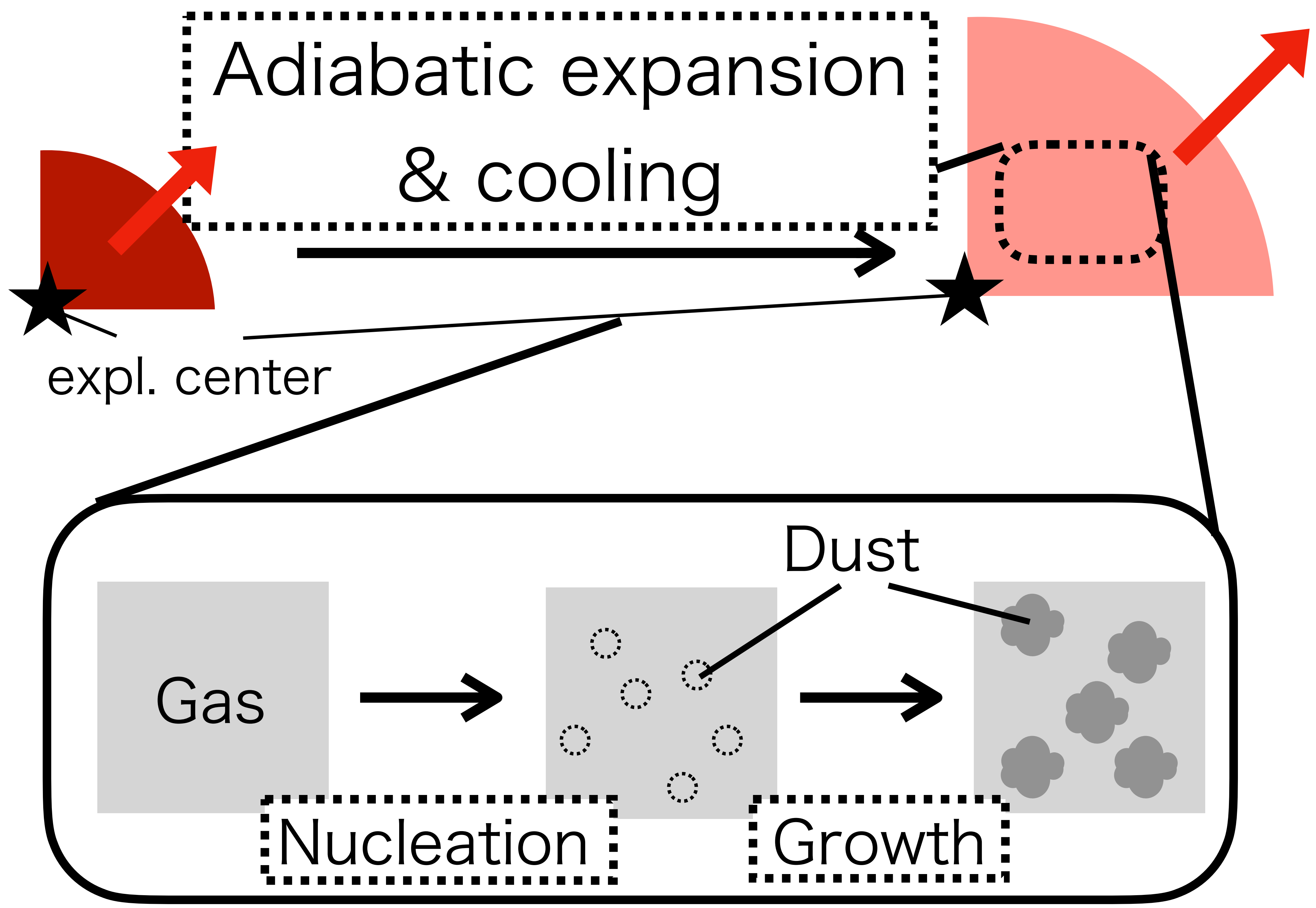

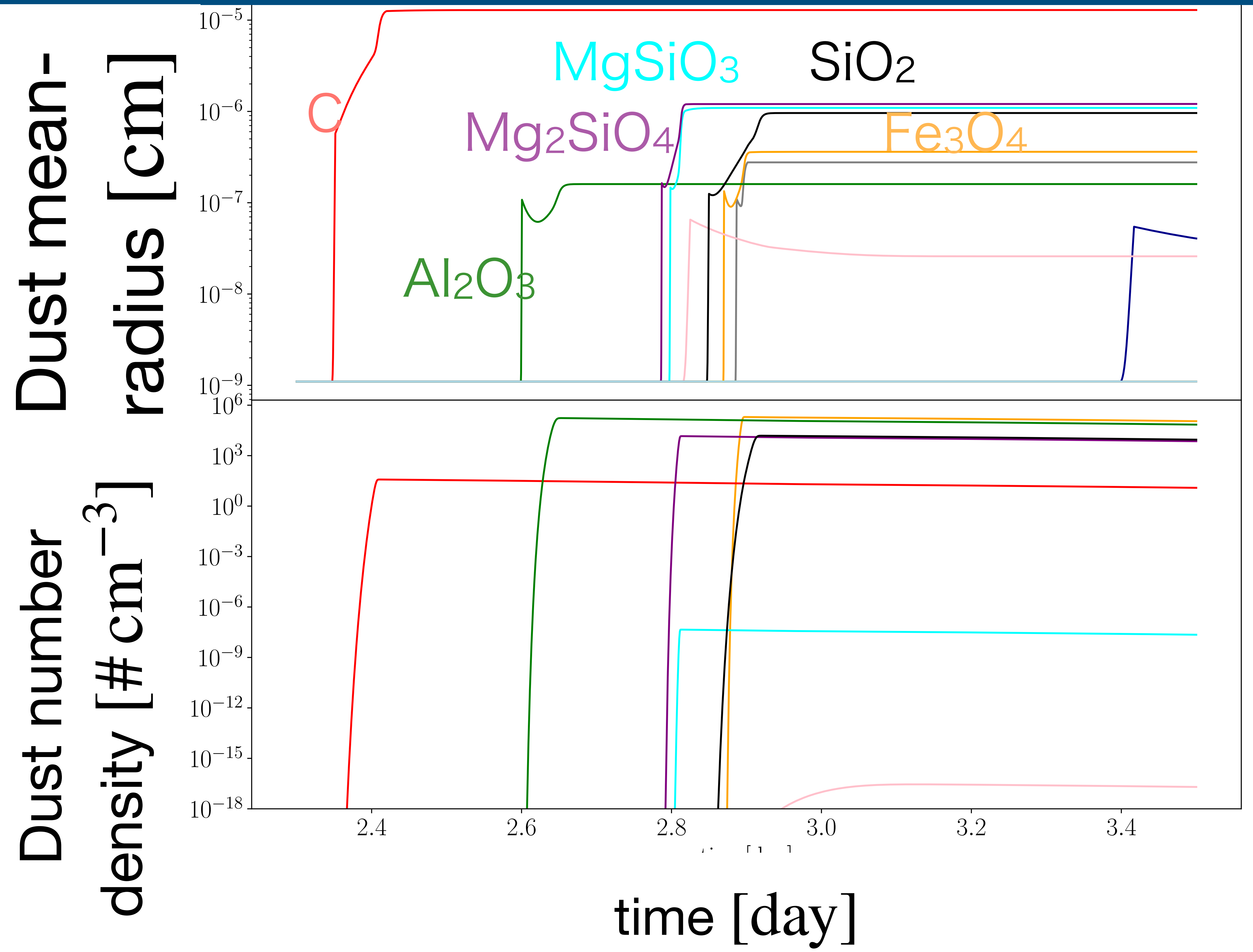

- Method: the thermal evolution of ejecta -> dust nucleation & growth model
- Result: C -> Al_2O_3 -> $MgSiO_3$ & Mg_2SiO_4 -> Fe_3O_4 -> SiO_2 ··· appeared
- More details in Poster 32!

Early warning from Eccentric compact Binaries

Multi-messenger astronomy!!

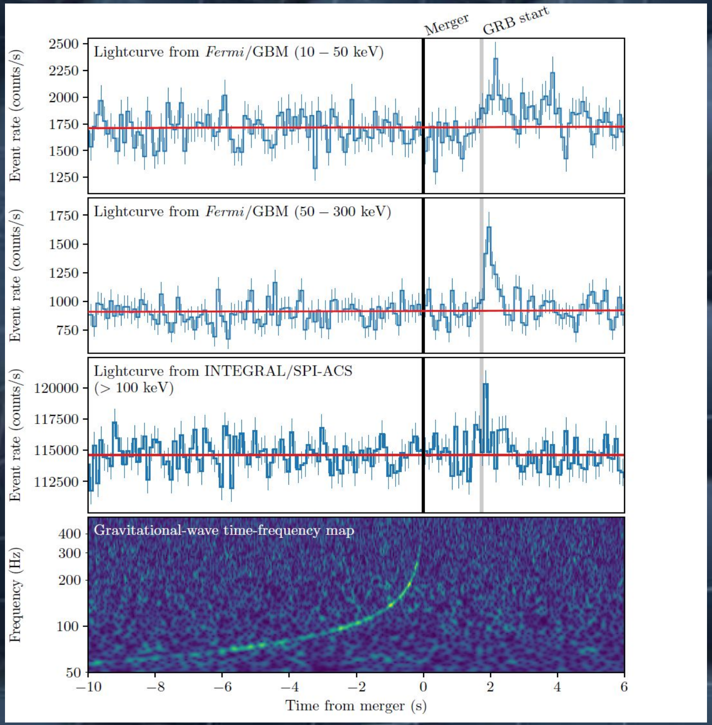

GW170817

LIGO-P1700308

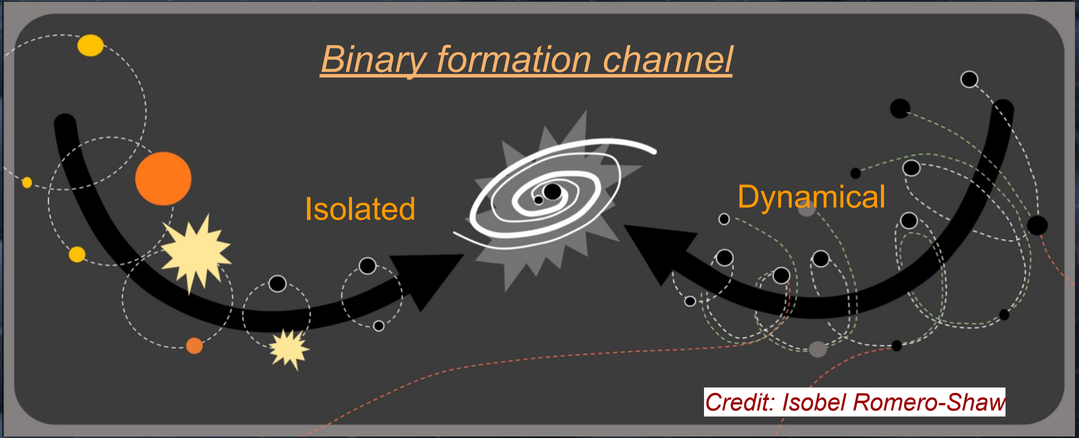

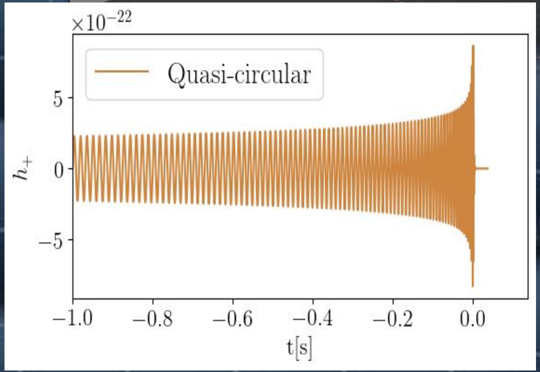

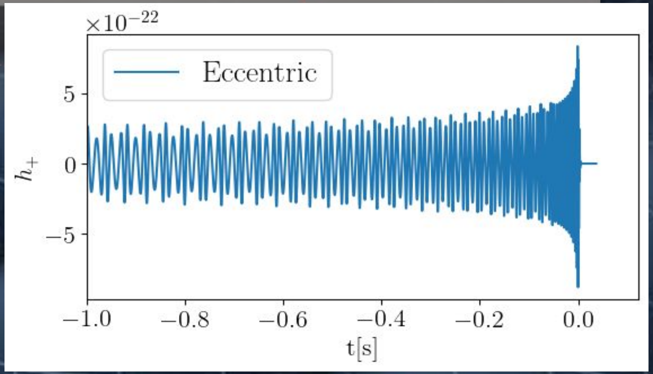

Template Initialization and Sub-dominant mode effects

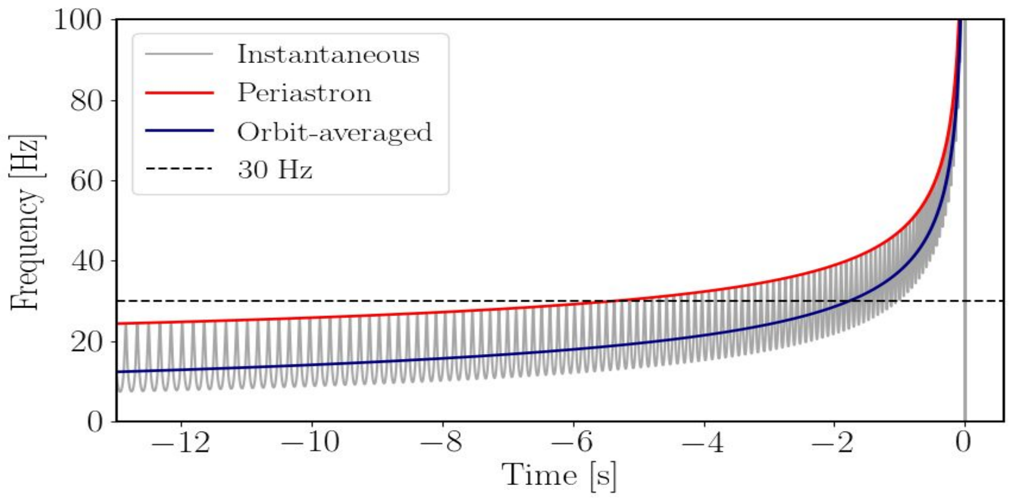

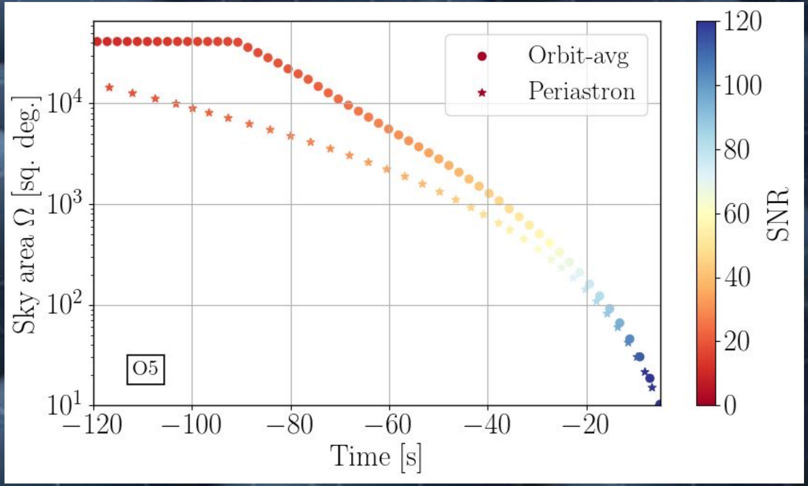

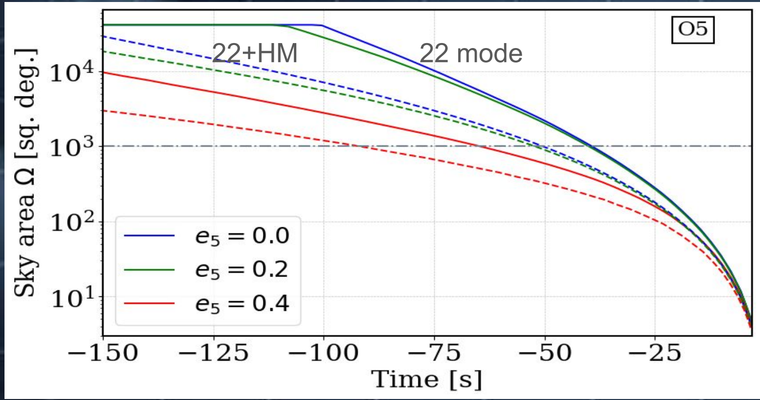

$$\bar{f^n} \equiv 4\int_0^\infty f^n \frac{|\tilde{h}(f)|^2}{S(f)} df$$

$$\sigma_t = \frac{1}{2\pi\rho\sigma_f}$$

Please visit Poster No. 33 for details...

P34

PINNs methods for the study of the magnetosphere of compact objects : Preliminary results

Matteo Stockinger, Alexis Reboul-Salze, Masaru Shibata

Short Poster Talk,
YKIS, February 13, 2025

- Magnetospheres important for emissions of compact objects
- We present a new method for the study of their global properties

MAX PLANCK INSTITUTE
FOR GRAVITATIONAL PHYSICS
(ALBERT EINSTEIN INSTITUTE)

Preliminary results

$$\partial_t \vec{E} = \nabla \times \vec{B} - \vec{j},$$

$$\partial_t \vec{B} = -\nabla \times \vec{E}, \qquad \vec{E} \cdot \vec{B} = 0.$$

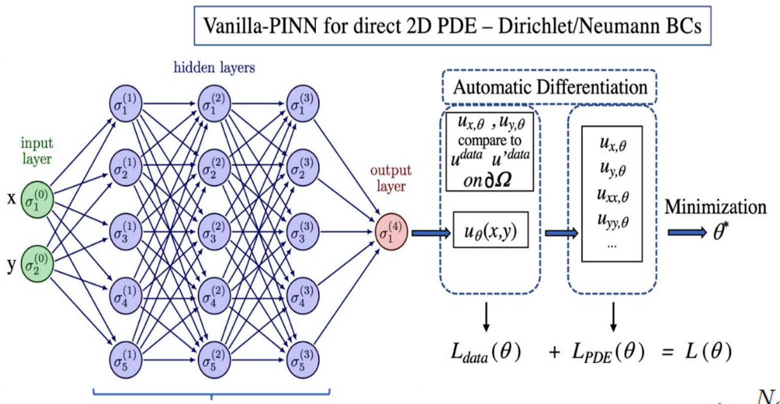

$$\mathcal{F}(u, x, \mu, u_x, \ldots) = 0, \quad x \in \Omega, \quad \mu \in \Omega_p, \quad L_{PDE}(\theta) = \frac{1}{N_c}\sum_{i=1}^{N_c} \left|\mathcal{F}(u_\theta(\boldsymbol{x_i}))\right|^2,$$

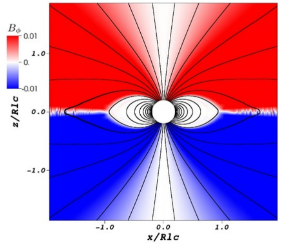

"onion code"
F. Carroso et al. 2018

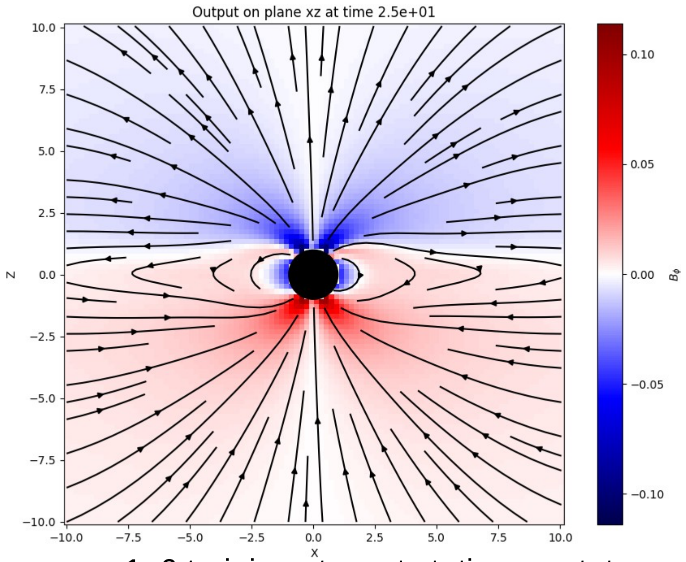

1e6 training pts, not stationary state

What Cosmic Explorer can do?

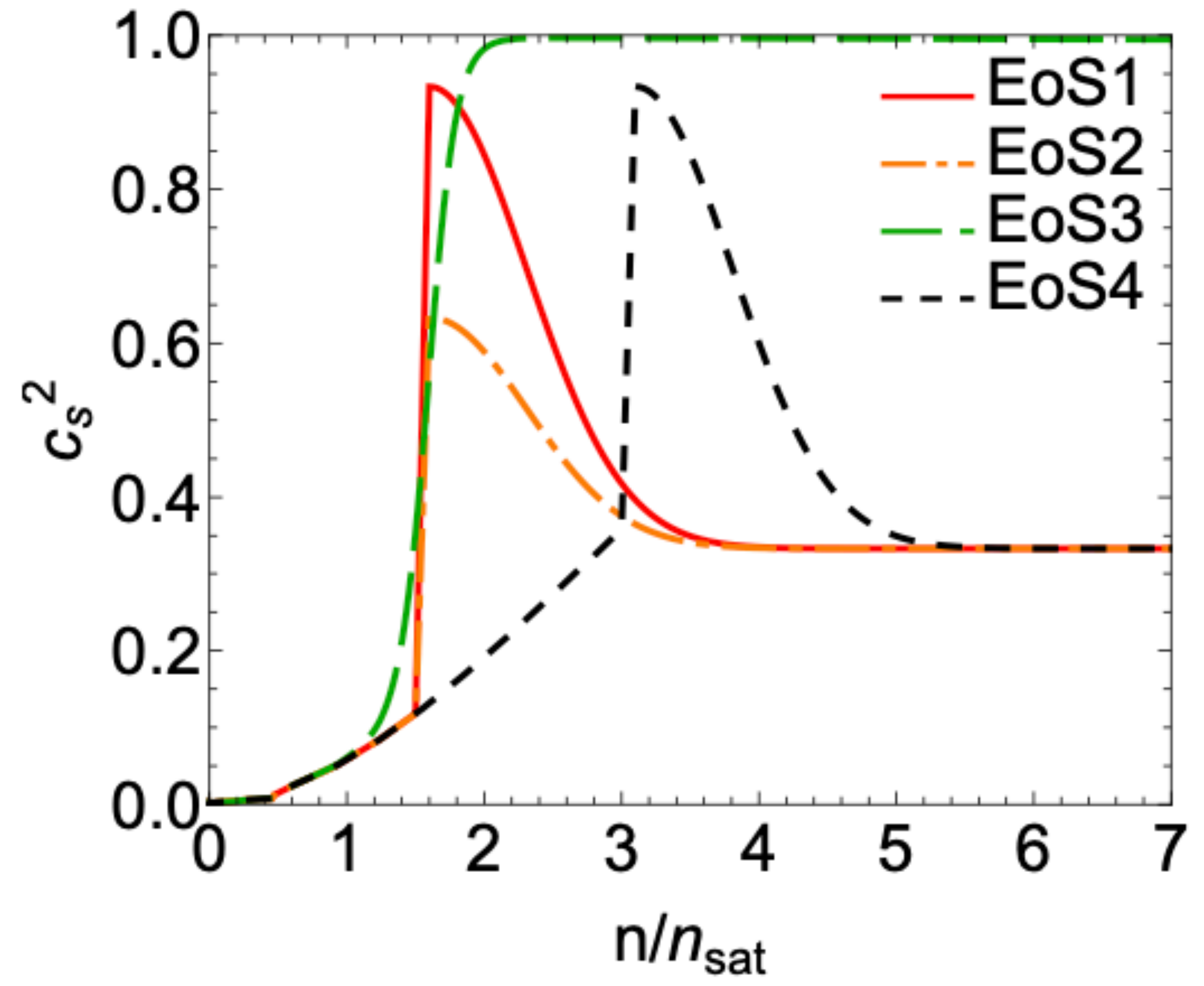

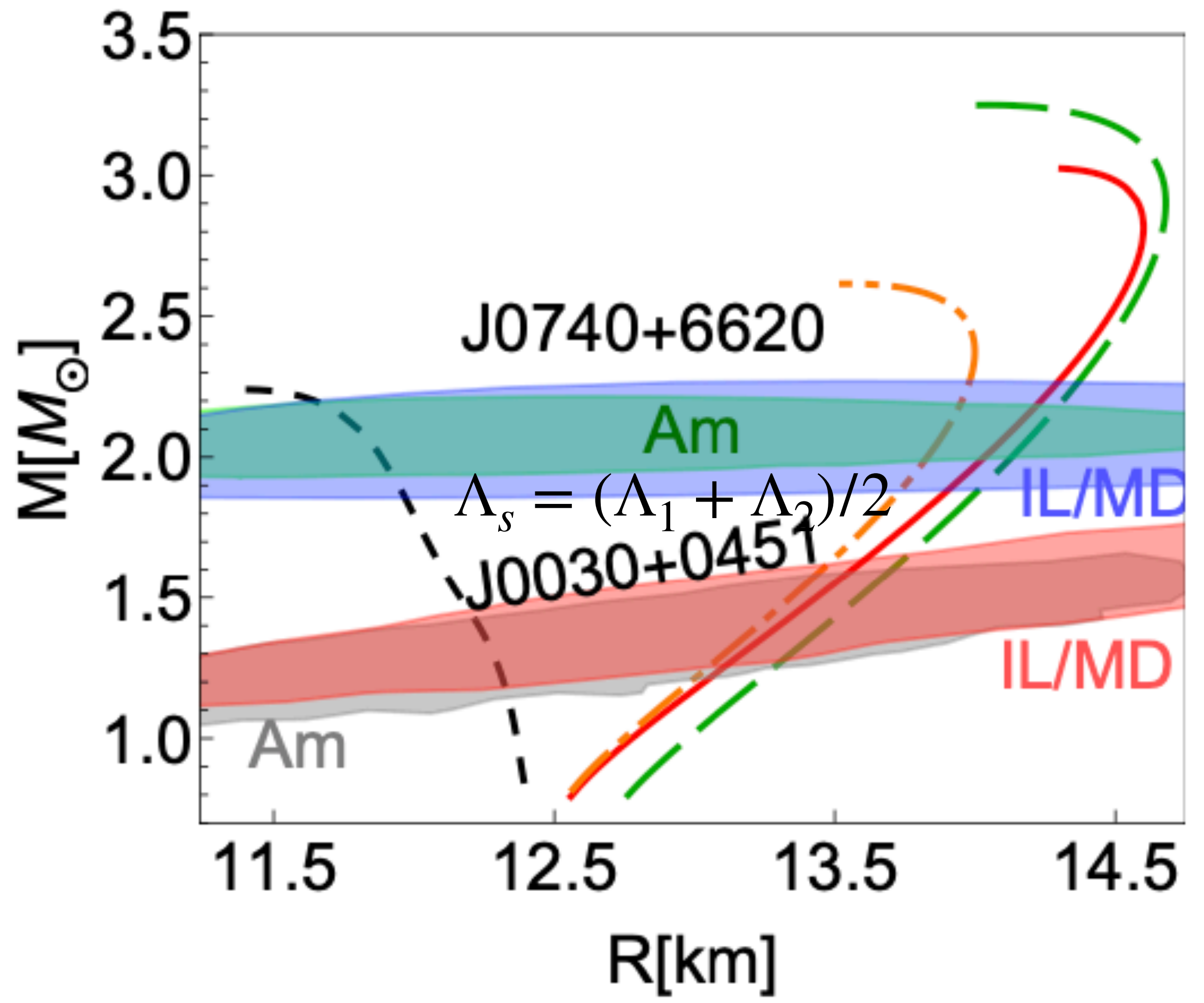

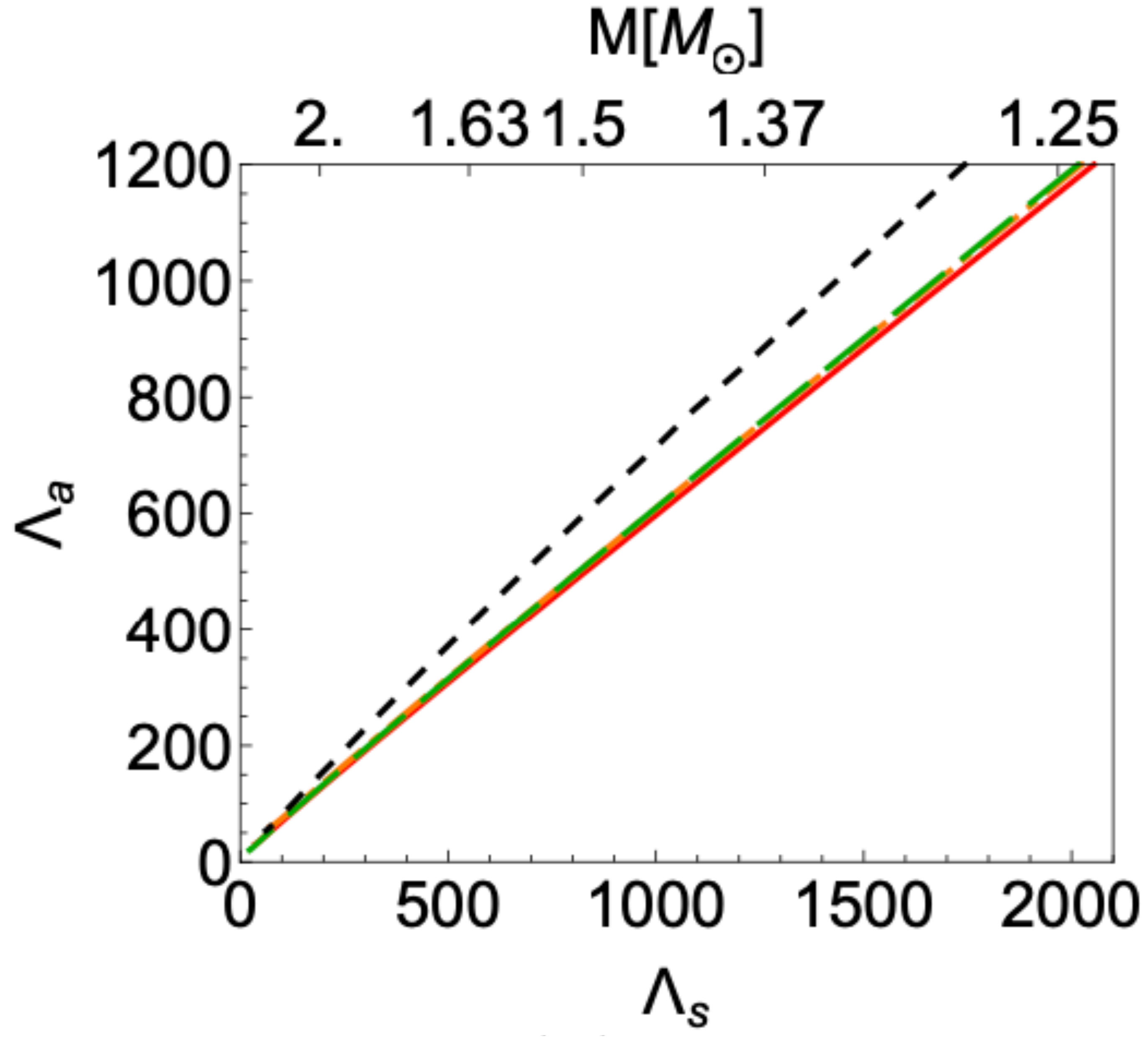

M_1/M_2 M_1/R_1

$$\frac{\Lambda_a}{\Lambda_s} = \frac{1-q^5}{1+q^5} - 10C_1\left(\frac{dR_1}{dM_1}\right)\frac{q^4(q-1)}{(q^5+1)^2} + \mathcal{O}(C_1^2)$$

EoS independent EoS dependent

- $\Lambda_s = (\Lambda_1 + \Lambda_2)/2$
- $\Lambda_a = (\Lambda_1 - \Lambda_2)/2$

What Cosmic Explorer can do?

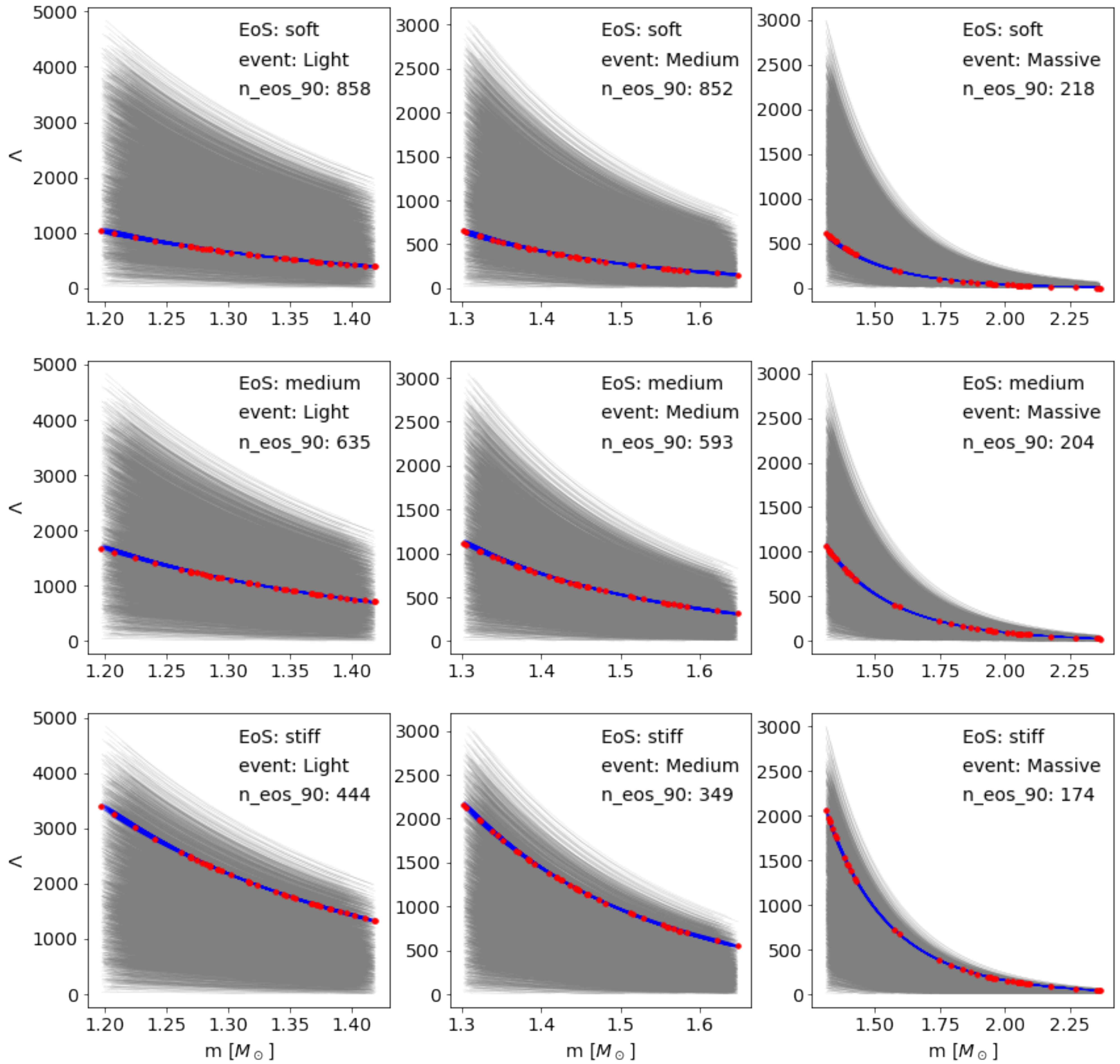

P36

Testing a Stochastic Acceleration Model of Pulsar Wind Nebulae: High-Energy Neutrino Emission

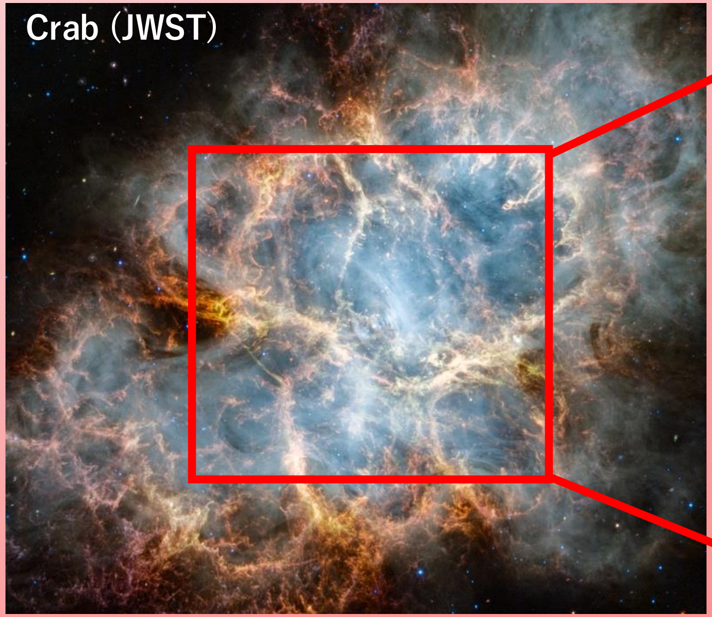

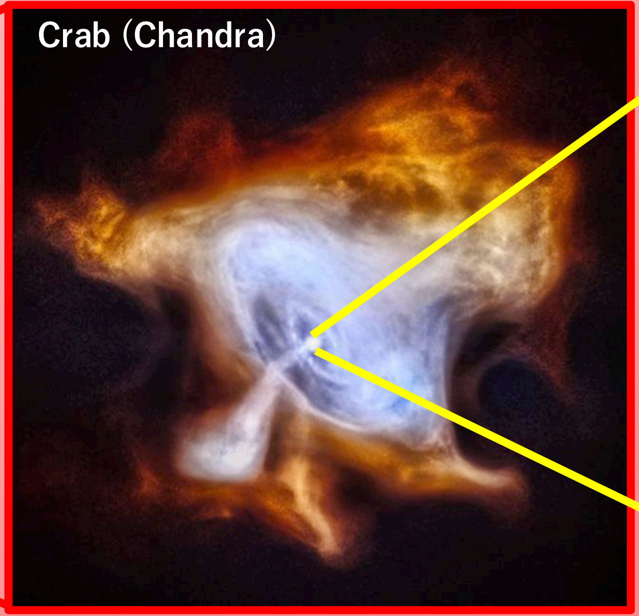

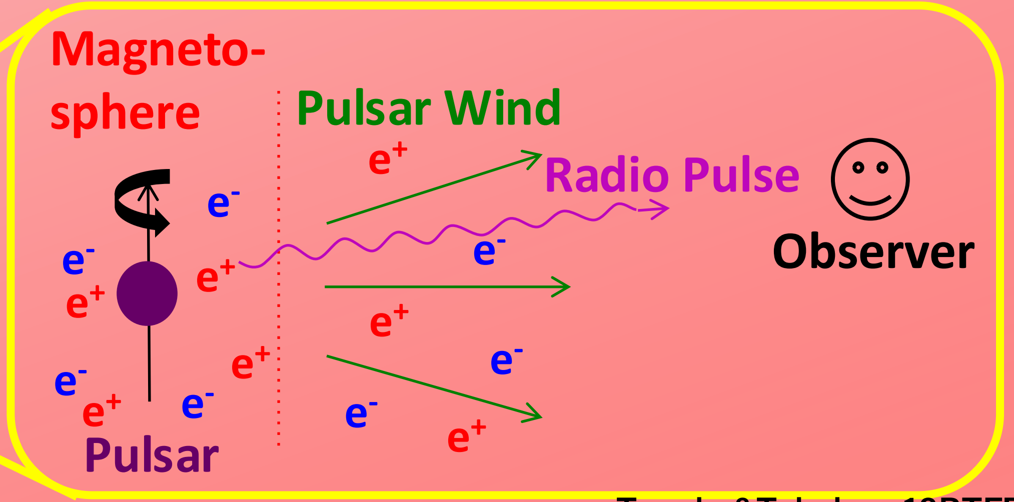

e.g., Tanaka&Takahara13PTEP

Shuta J. Tanaka
(Aoyama Gakuin University)

Particles from the filaments + stochastic acceleration
↓
radio and > PeV emission + neutrinos

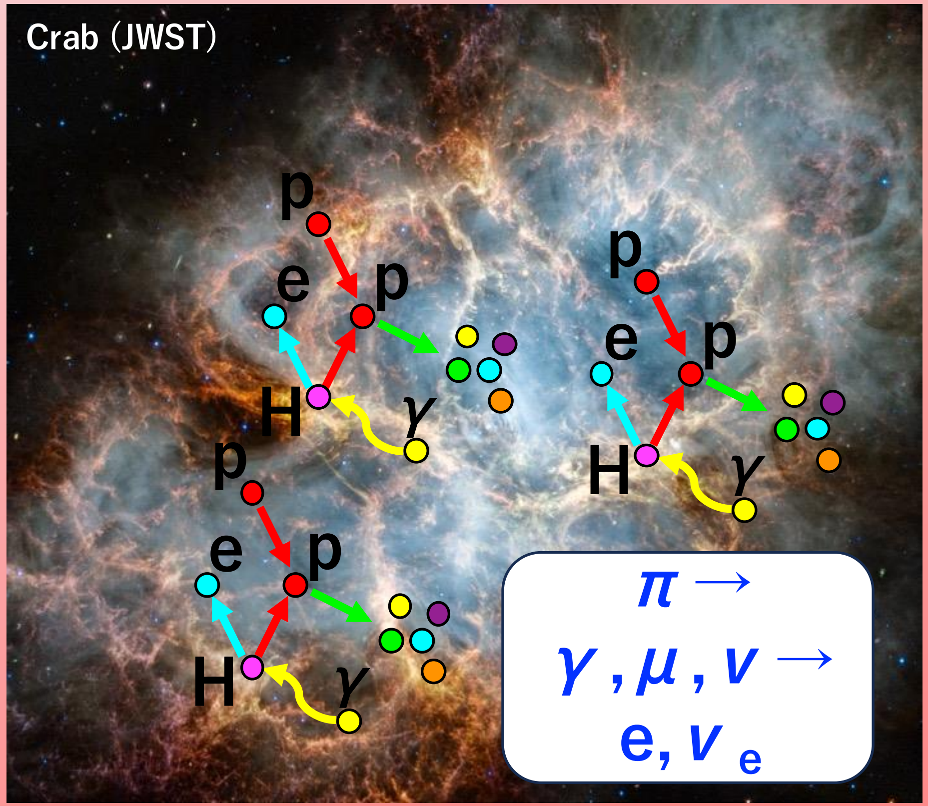

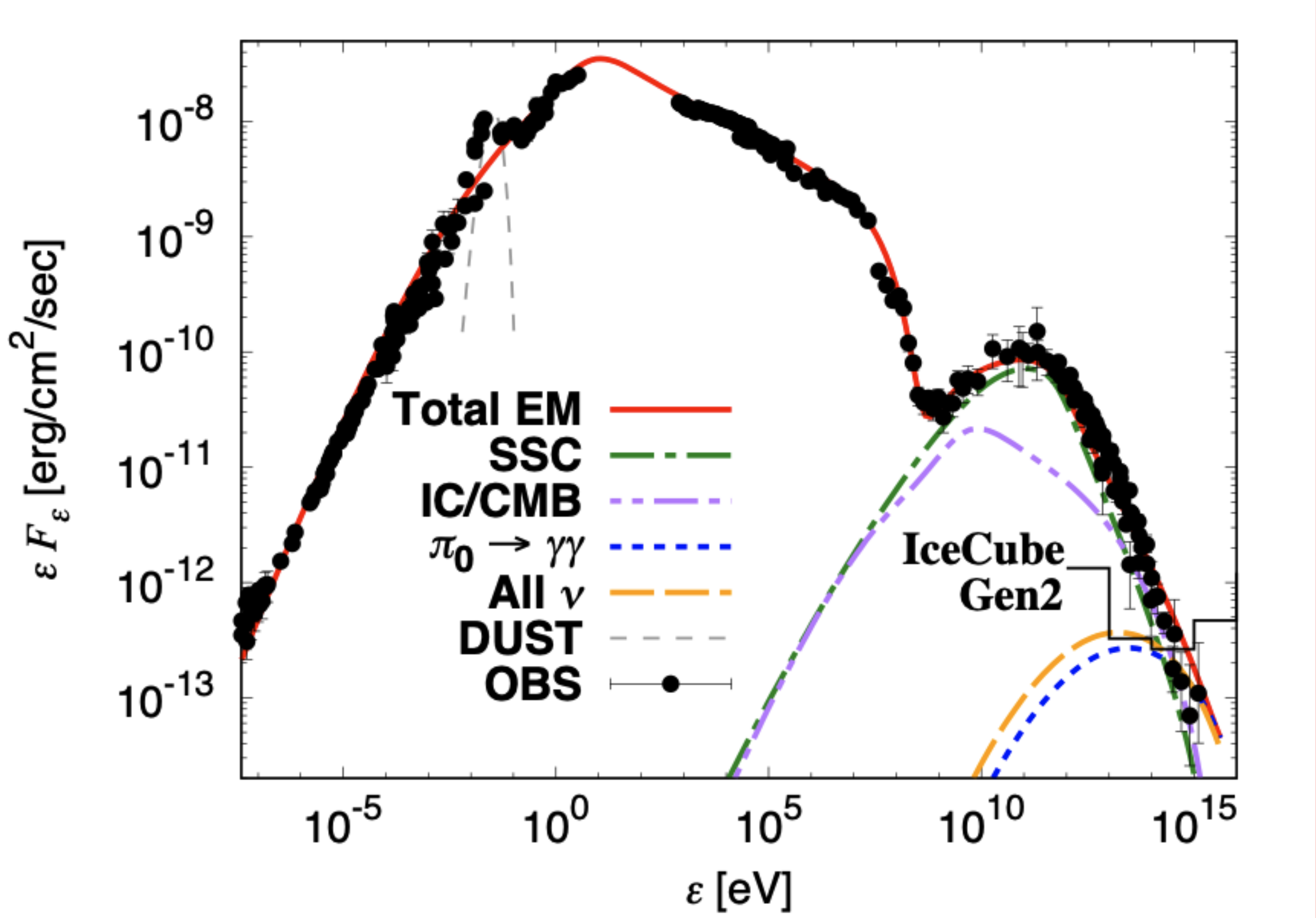

P37 Seiji Toshikage (Tohoku)

Optical Transient Counterpart Search for IceCube High-energy Neutrino Events

GOAL: Testing explosive transients as sources of high-energy particles

IceCube is sensitive to neutrino sources in the distant Universe (z ≦ 2)

-> requires large telescopes + heavily contaminated by unrelated SNe

💡 Multiple neutrino detections -> nearby (z ≦ 0.2) transient source! Yoshida+2022

This work: the first optical search for an IceCube multiple-neutrino event

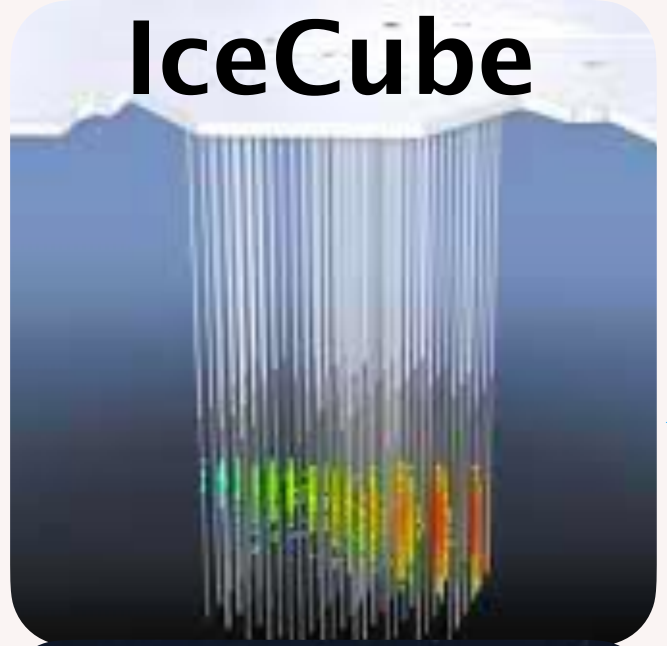

Triple neutrinos within 16 days!

IceCube 2025

ZTF serendipitously observed the same region

Toshikage et al. 2025

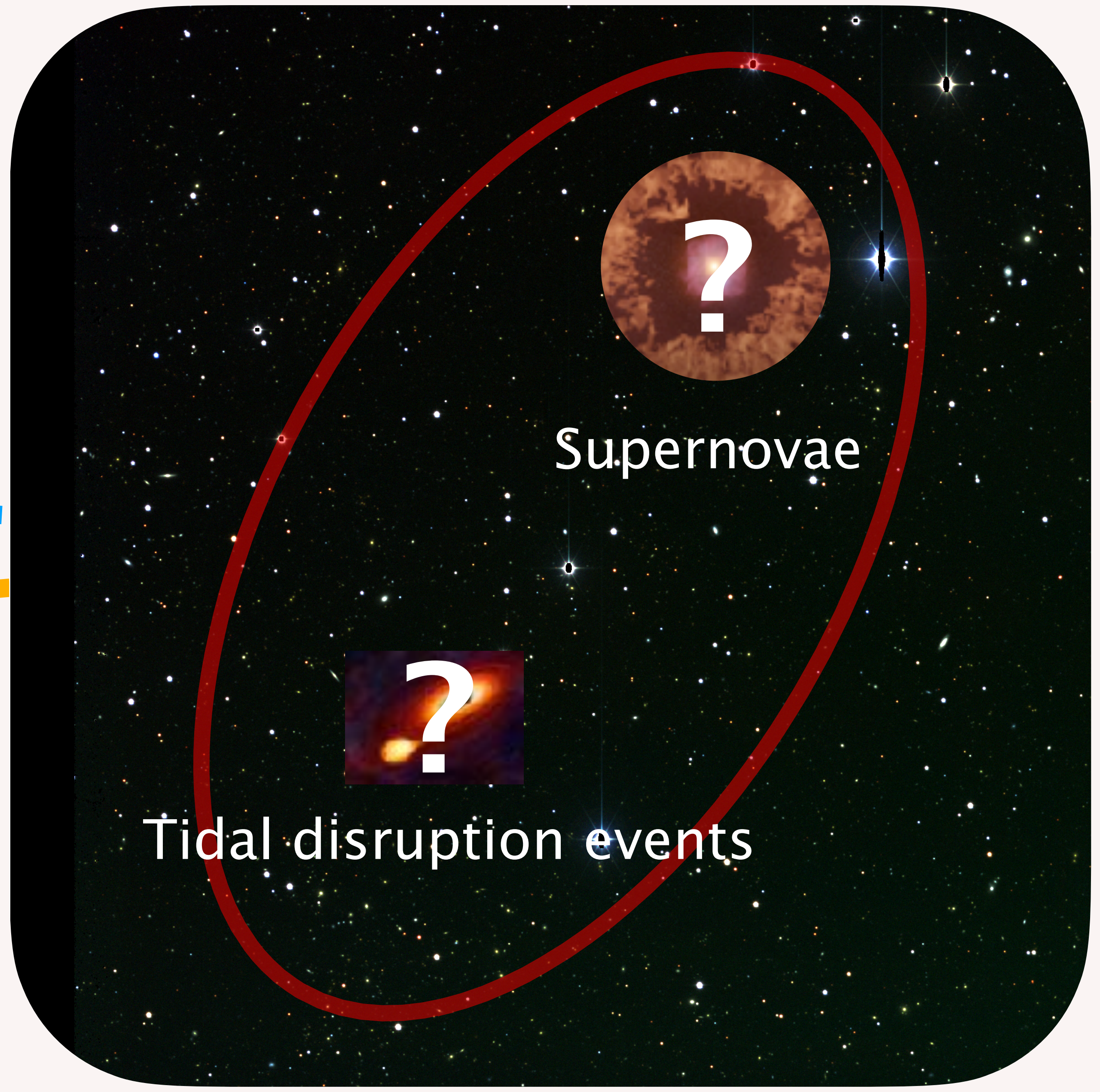

Were there any neutrino source candidates in that direction ?

Optical Transient Counterpart Search for IceCube High-energy Neutrino Events

Dedicated analysis of the optical data using a blind analysis

✔ confirm that SNe or TDEs are readily detectable if they are the main source of neutrinos

No optical counterparts were identified

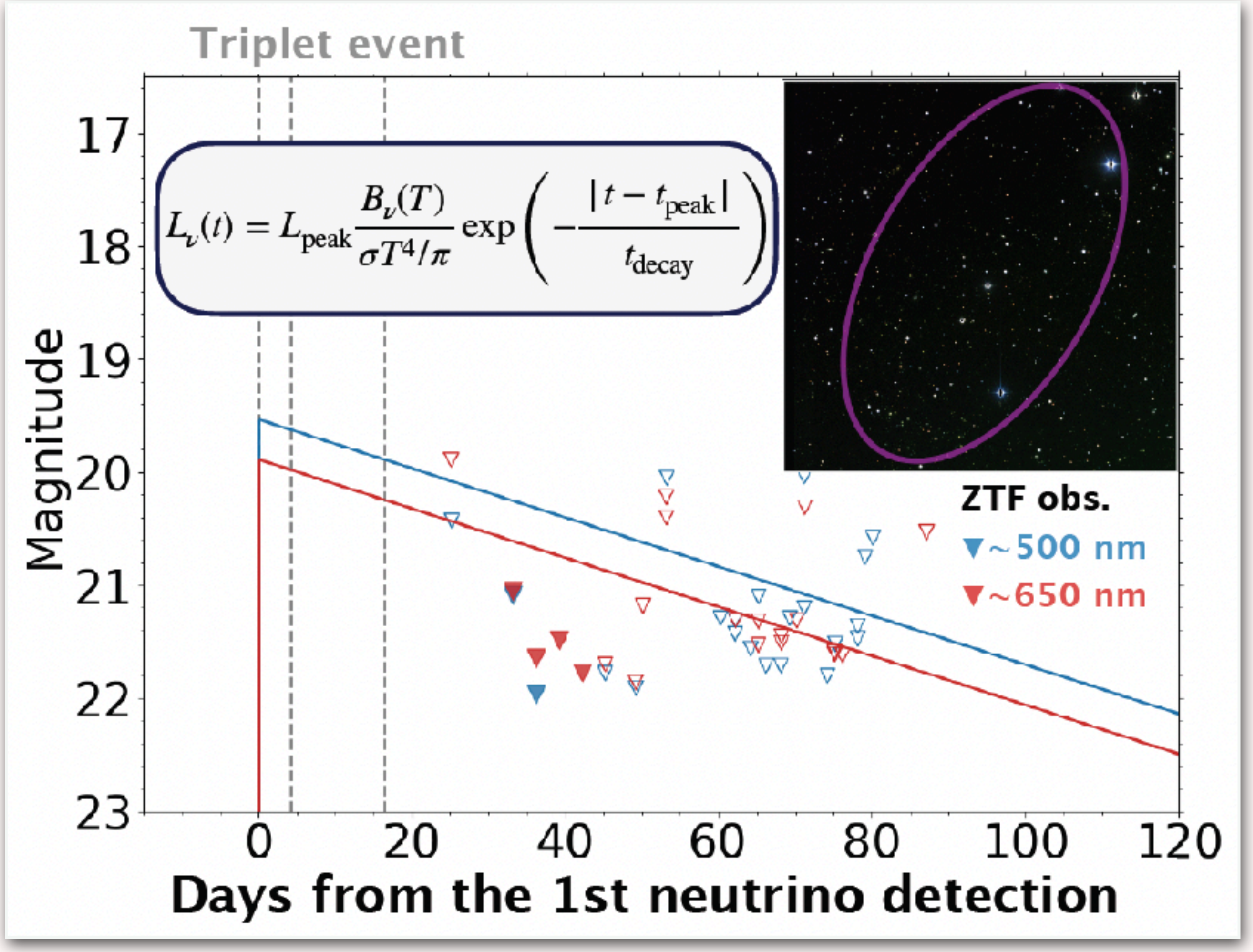

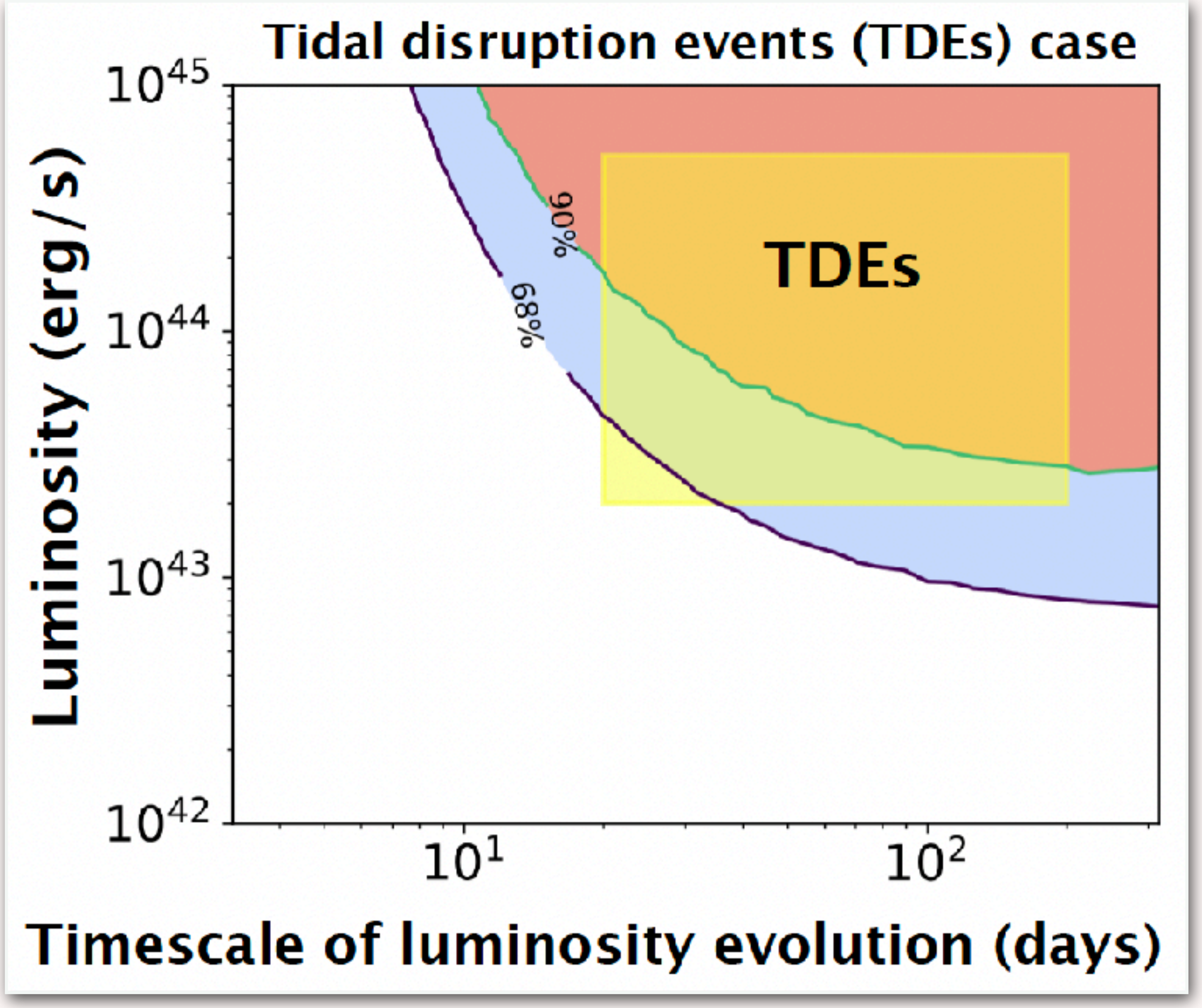

Follow-up for multiplets can place strong constraints on source properties

P38

Evolutionary pathways of long-period cataclysmic variables: a bridge to AM CVn systems, Type Ia supernovae, and gravitational waves

Gagik Tovmassian, Ivan Mora, Juan Echevarría – Instituto de Astronomía, UNAM, Mexico
Diogo Belloni – ICESUN, Yunnan Key Laboratory of Supernova Research, Yunnan Observatories, China

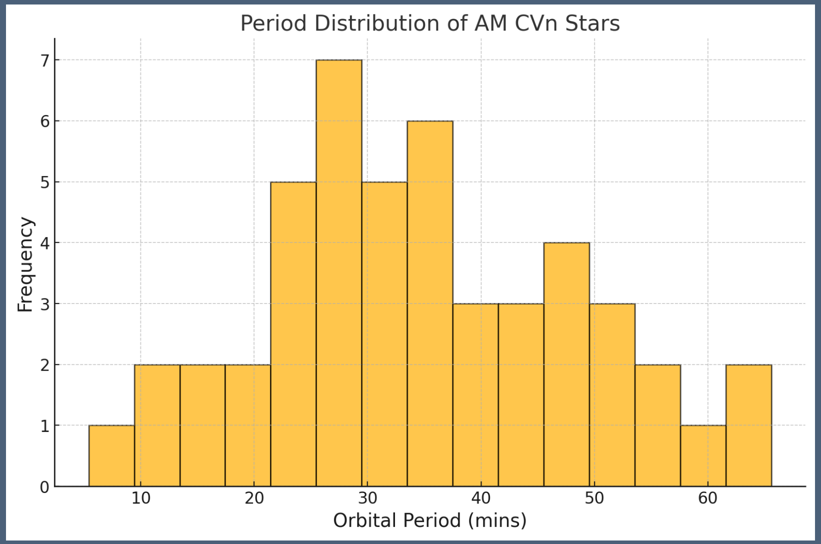

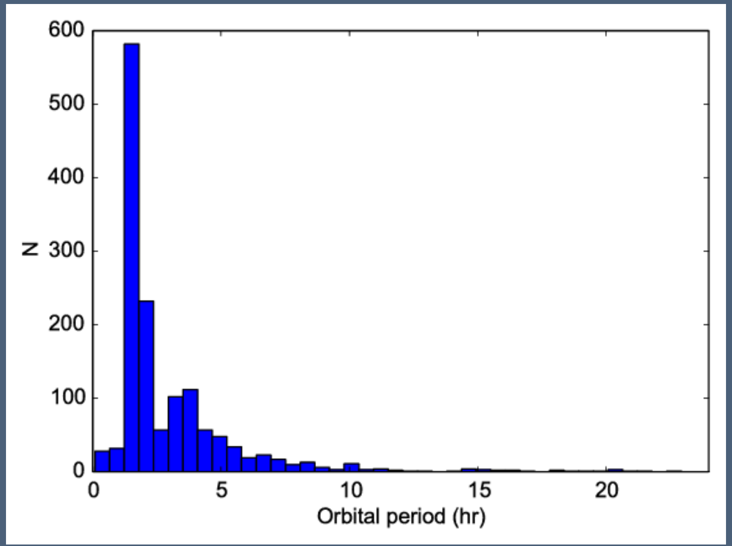

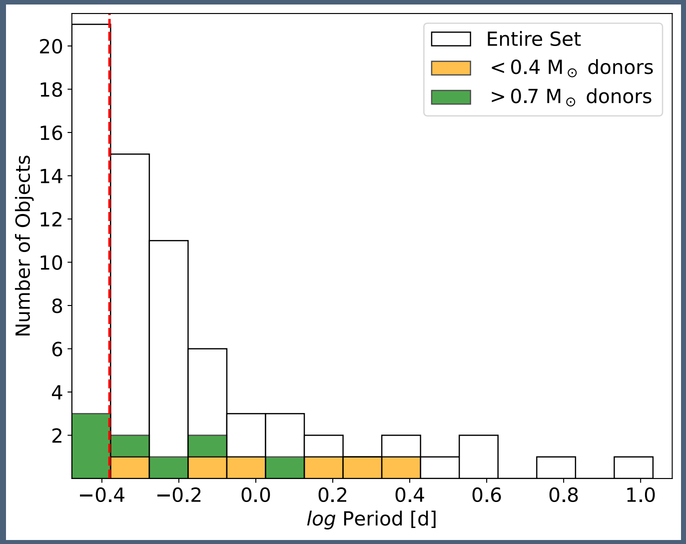

More recent studies have shown that the hydrogen-rich CV channel can be significantly more efficient if angular-momentum losses are enhanced during thermal-timescale mass transfer. In particular, the consequential angular momentum loss (CARB) model proposed by van & Ivanova (2019) predicts substantially accelerated evolution, allowing evolved long-period CVs to rapidly shed their hydrogen envelopes and evolve into AM CVn systems, as illustrated in Fig. 4 of Belloni & Schriber (2023).

Belloni, D. and Schreiber, M. R.: A&A 678, A34 (2023)

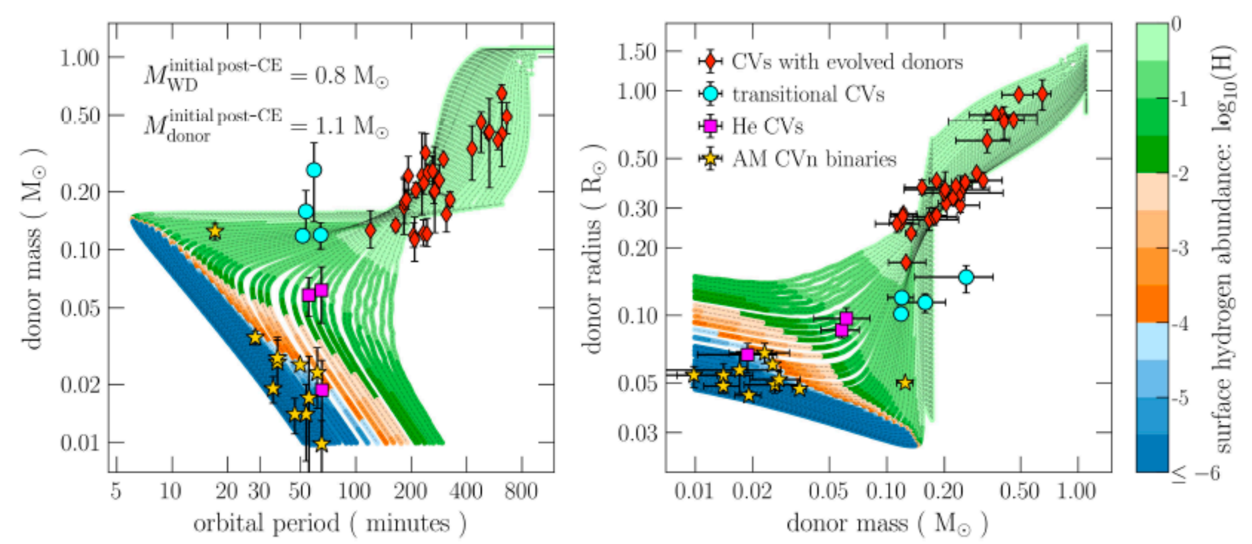

Fig. 4. Convergent CV evolution when the CARB model for magnetic braking is adopted for different initial post-CE binaries. The colour represents the log-scaled surface hydrogen abundance of the donor. Systems can be considered as AM CVn binaries if they reach shades of blue. Related objects, that is, CVs, transitional CVs, and He CVs are indicated by shades of other colours. While the assumed initial post-CE orbital periods cover values from 1.98 to 3.00 d, we fixed the initial post-CE white dwarf mass to 0.8 $M_\odot$ and the initial post-CE companion mass to 1.1 $M_\odot$. The evolution of the surface hydrogen abundance is strongly dependent on the mass of the helium core at the onset of mass transfer: the more massive the helium core, the lower the surface hydrogen abundance at a given orbital period during post-orbital-period-minimum evolution. CVs with donors having initially less massive helium cores bounce at longer orbital periods, leading to more massive and larger donors during AM CVn binary evolution. Along with the evolutionary tracks we included the following observed systems: CVs harbouring nuclear evolved donors (red diamonds), transitional CVs (cyan circles), He CVs (magenta squares), and AM CVn binaries (yellow stars), as described in Sect. 2.4. Except for AM CVn itself, the one with largest donor mass among AM CVn binaries, the characteristics of all AM CVn binaries can be explained by the CV channel, which means that the lack of hydrogen lines in the optical spectra of AM CVn binaries cannot be easily used as an argument against the CV formation channel. See Sect. 4.1 for more details.

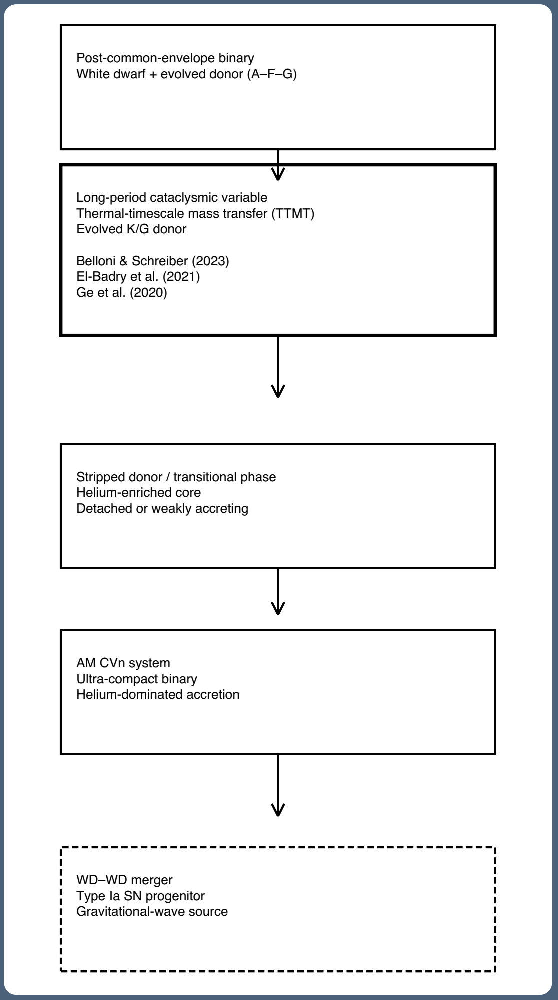

V479 And Porb ≃ 0.594 d

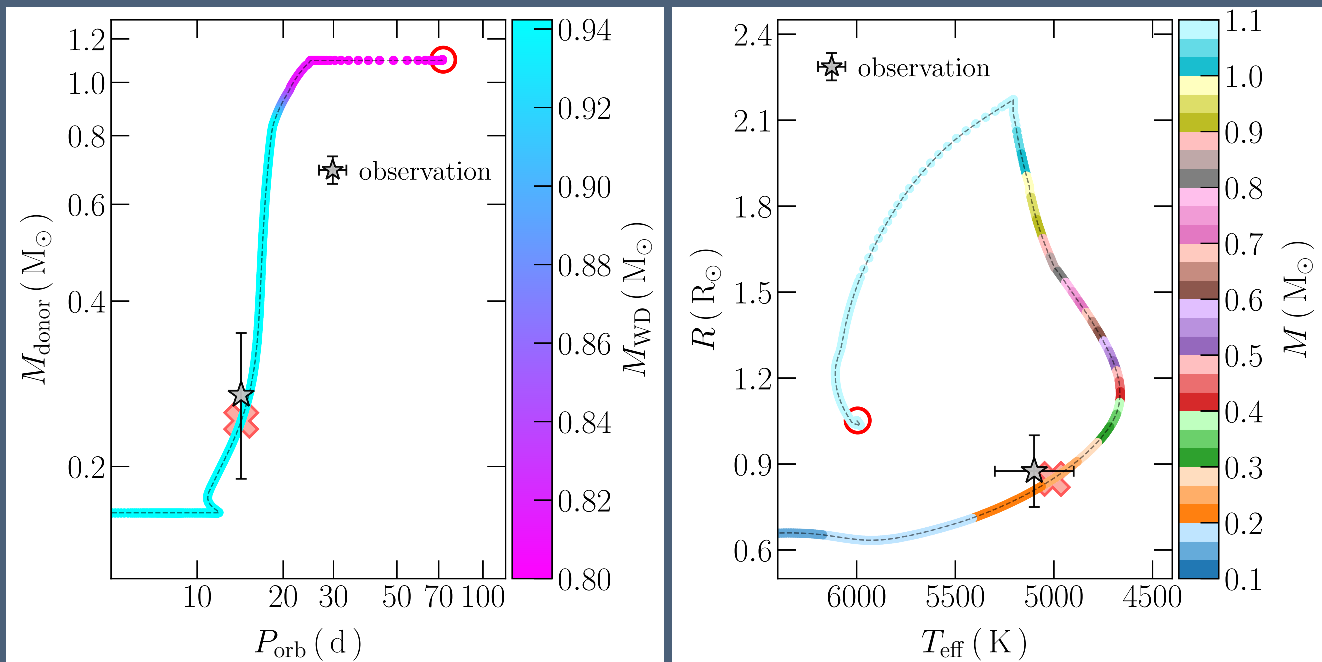

V1082 Sge Porb = 0.868 d

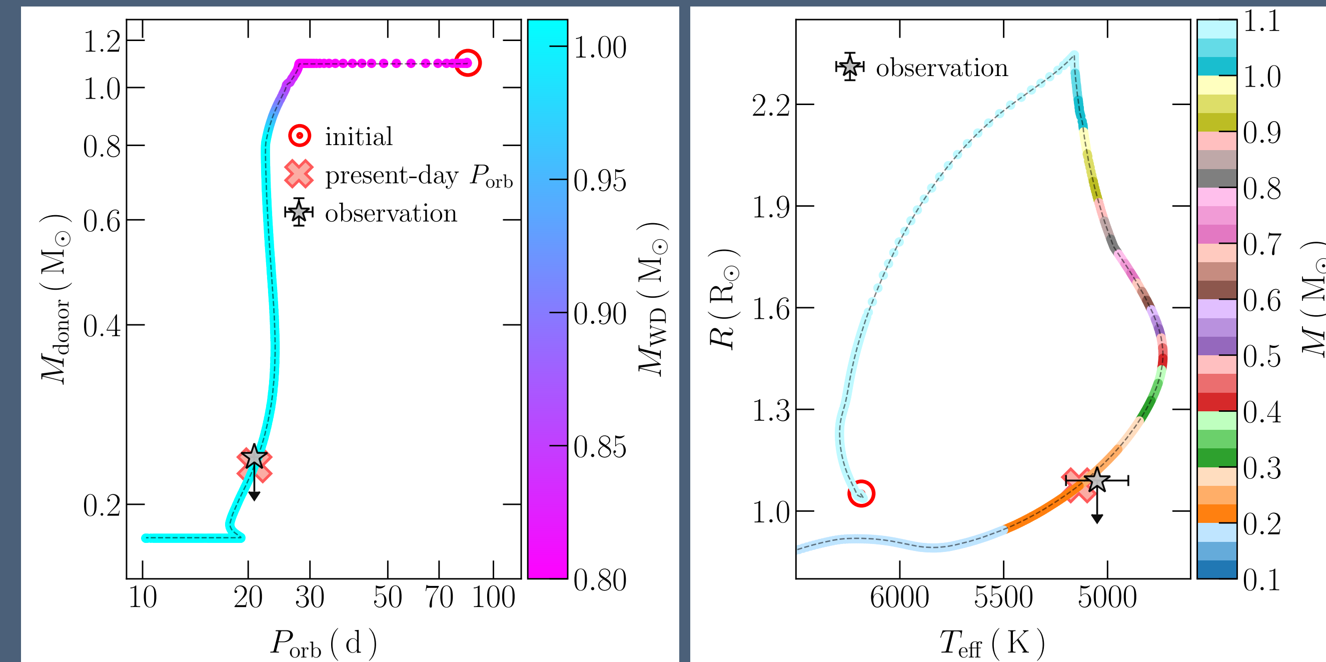

SDSS J085210.48+783246.6 Porb ≃ 0.7129 d

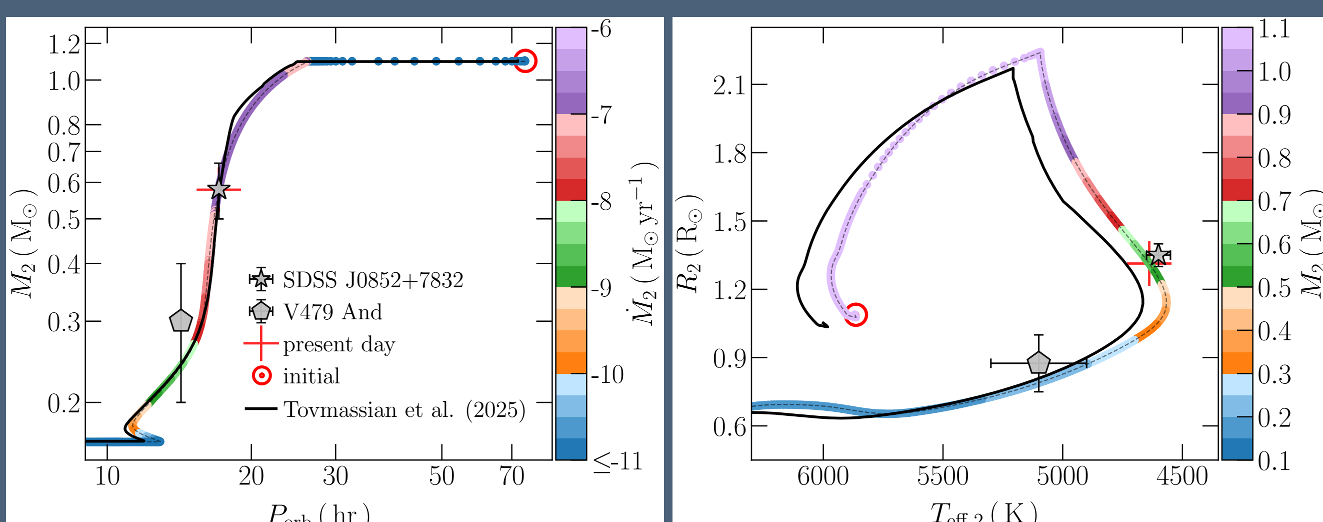

V630 Cas Porb ≃ 2.5638 d

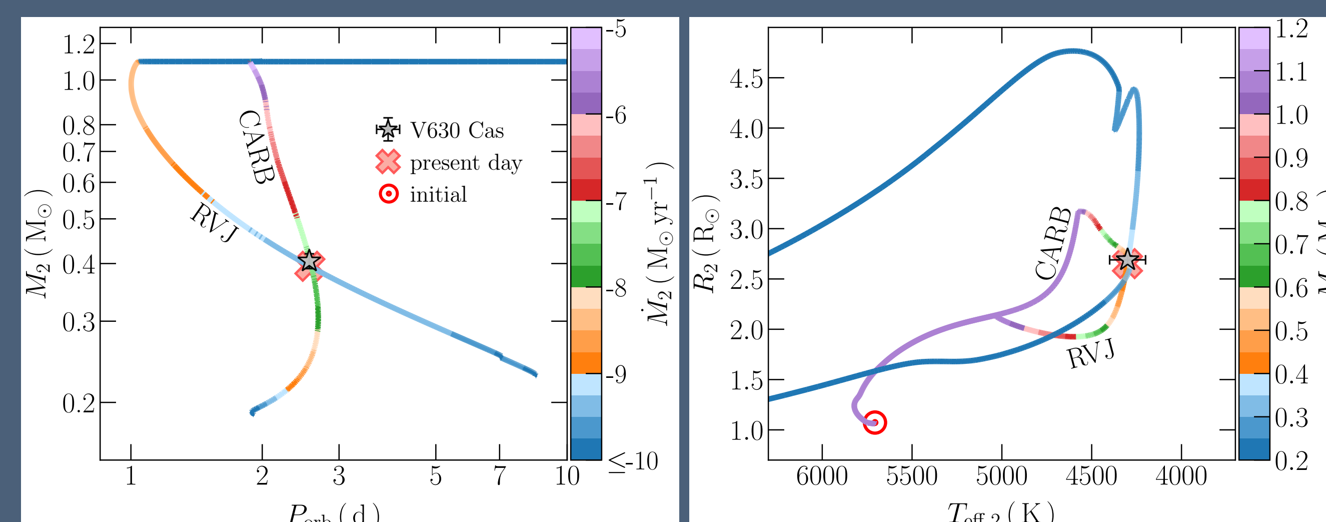

Conclusions

Long-period cataclysmic variables provide compelling evidence that standard CV evolutionary pathways are incomplete. Systems listed here consistently require undermassive but inflated donor stars, whose positions on mass–radius and HR-like diagrams can only be explained if significant nuclear evolution preceded the onset of mass transfer. The agreement between observed system parameters and evolutionary tracks demonstrates that these binaries evolve through non-canonical channels, often characterized by thermal-timescale or otherwise unstable mass transfer and, at long periods, diverging orbital evolution.

Crucially, these systems occupy a natural evolutionary bridge between hydrogen-rich CVs and hydrogen-deficient compact binaries. As mass transfer proceeds, donors are progressively stripped of their hydrogen envelopes, leaving low-mass helium cores that are expected to evolve into helium white dwarfs, producing double-degenerate binaries. In this framework, some long-period CVs with evolved donors represent progenitors of AM CVn-like systems, linking observable present-day binaries to populations relevant for compact binary evolution.

Multiphase shock cooling in ultra-stripped supernovae

Samantha Wu, Carnegie Observatories (with Annastasia Haynie, Tony Piro, Jim Fuller)

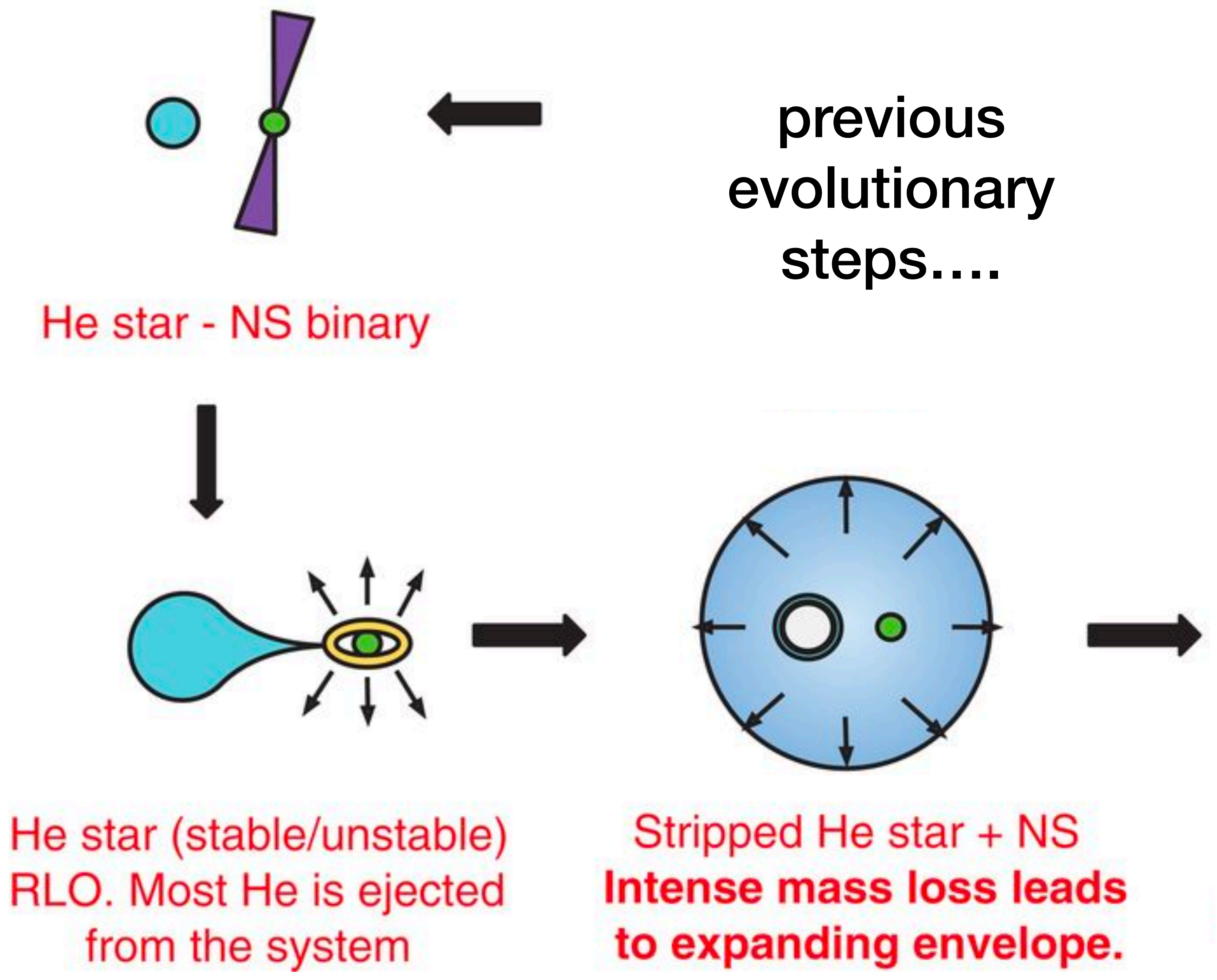

previous evolutionary steps....

from De et al. 2018

Final supernova (SN):

ultra-stripped SN or SN Ibn surrounded by circumstellar material (CSM)

MESA binary models
→ final He star mass, mass loss rates for CSM
→models of SN progenitors

extended He envelope $\sim 0.4 - 1\,M_\odot$

+

CSM $\sim 0.001\,M_\odot$ to $\sim 0.1\,M_\odot$

What do light curves of SNe from binary stripped star + CSM progenitors look like?

Multiphase shock cooling in ultra-stripped supernovae

Samantha Wu, Carnegie Observatories

Please come by poster 39 to learn more!

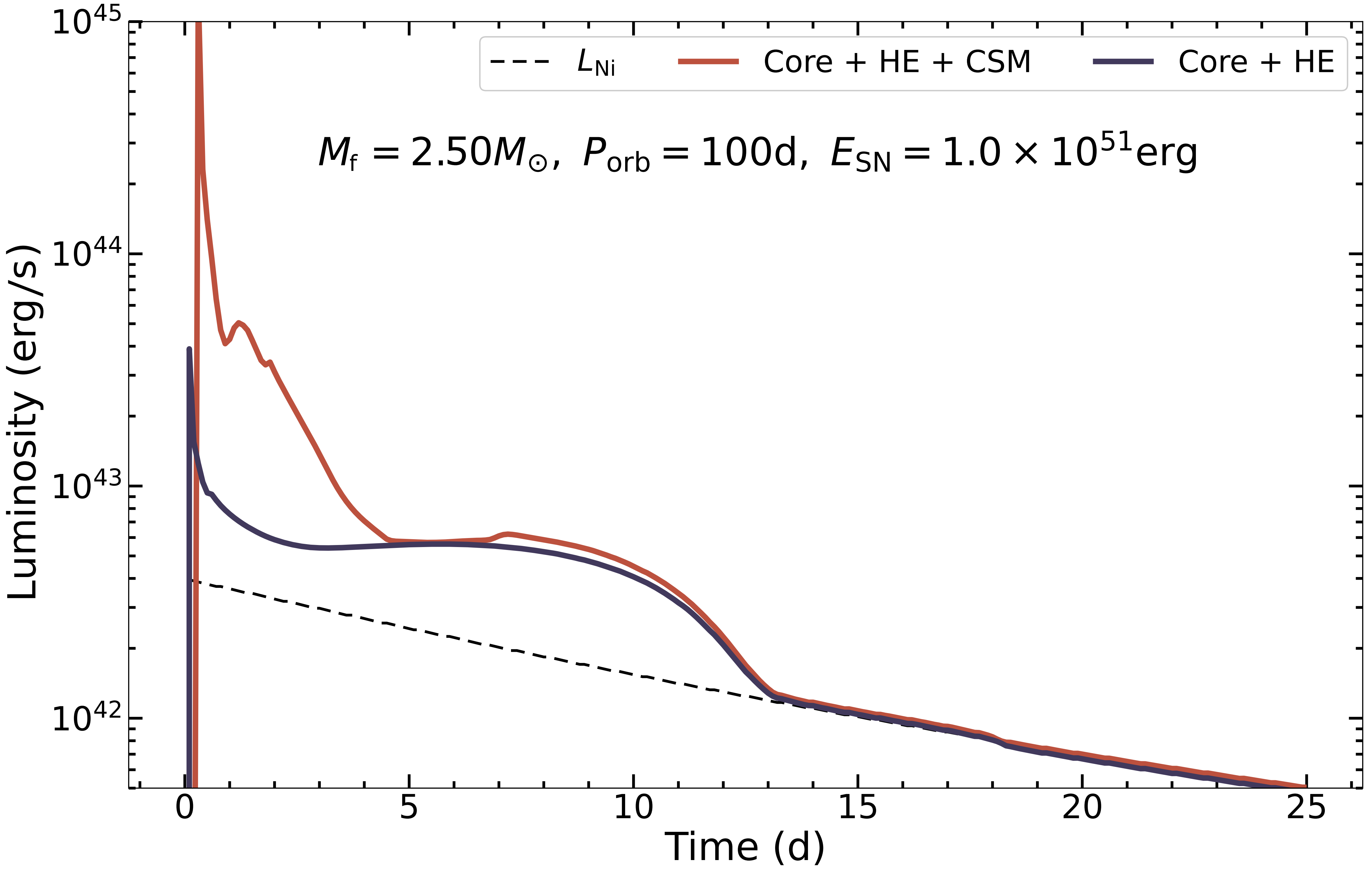

Good fit to observed ultra-stripped SN

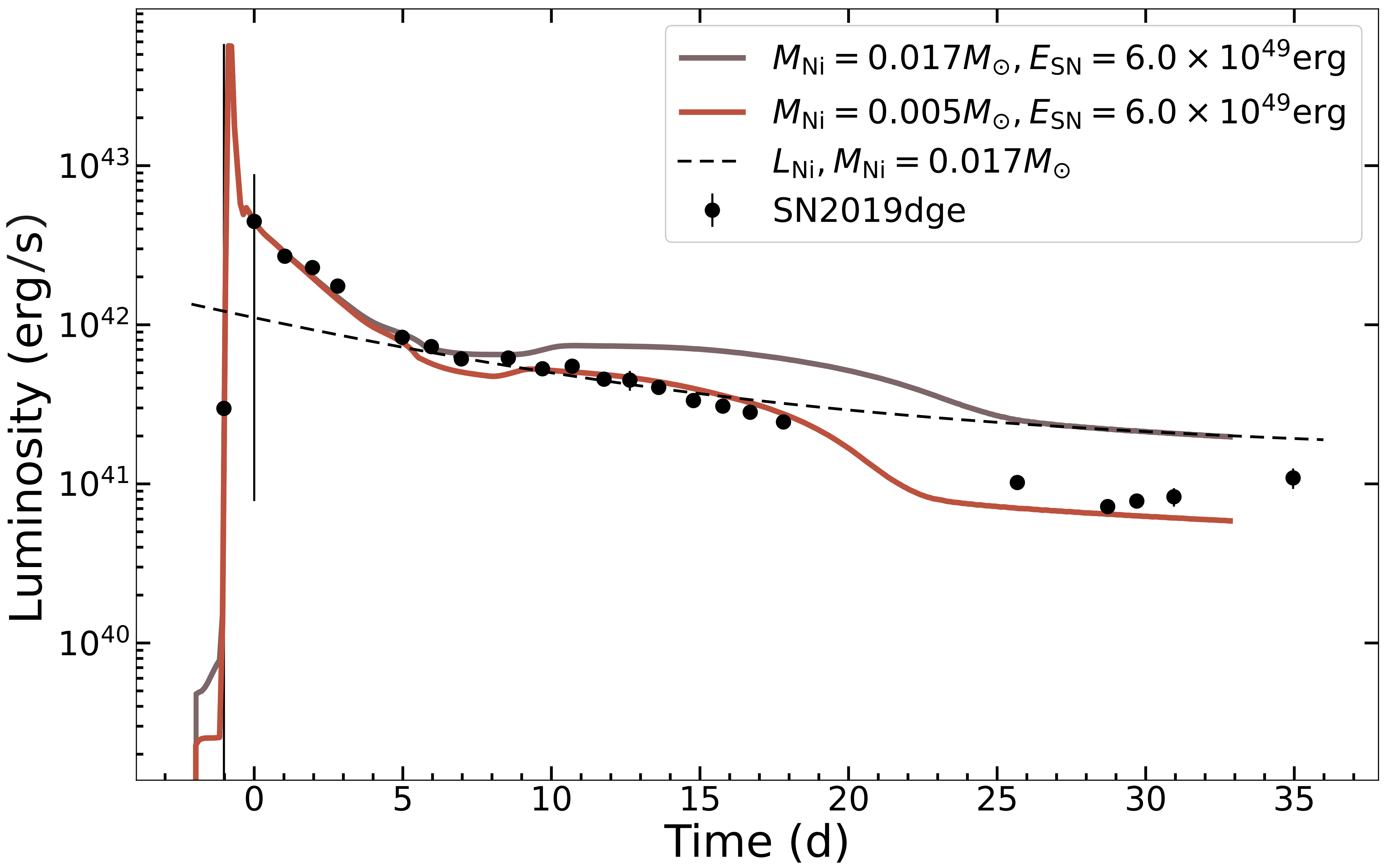

Shock cooling from **CSM** and from **extended helium envelope** both contribute to early time light curve